

2018-01-01

CRISPR/Cas9-Induced Genetic Disruption and Characterization of UDP-Galactopyranose Mutase In Trypanosoma Cruzi

Claudia Manriquez

University of Texas at El Paso, cmanriquezroman@miners.utep.edu

Follow this and additional works at: https://digitalcommons.utep.edu/open_etd



Part of the [Molecular Biology Commons](#), and the [Parasitology Commons](#)

Recommended Citation

Manriquez, Claudia, "CRISPR/Cas9-Induced Genetic Disruption and Characterization of UDP-Galactopyranose Mutase In Trypanosoma Cruzi" (2018). *Open Access Theses & Dissertations*. 1475.
https://digitalcommons.utep.edu/open_etd/1475

This is brought to you for free and open access by DigitalCommons@UTEP. It has been accepted for inclusion in Open Access Theses & Dissertations by an authorized administrator of DigitalCommons@UTEP. For more information, please contact lweber@utep.edu.

CRISPR/CAS9-INDUCED GENETIC DISRUPTION AND CHARACTERIZATION OF
UDP-GALACTOPYRANOSE MUTASE IN
TRYPANOSOMA CRUZI

CLAUDIA MANRIQUEZ ROMAN
Master's Program in Biological Sciences

APPROVED:

Igor C. Almeida, D.Sc., Chair

Rosa A. Maldonado, D. Sc.

German Rosas-Acosta, Ph.D.

Katja Michael, Ph.D.

Charles Ambler, Ph.D.
Dean of the Graduate School

Copyright ©

by

Claudia Manriquez Roman

2018

Dedication

*To my mother Alma Rosa Roman Salcedo and my father Jose Ricardo Manriquez Zamudio for
your endless amount of love and unconditional support.*

CRISPR/CAS9-INDUCED GENETIC DISRUPTION AND CHARACTERIZATION OF
UDP-GALACTOPYRANOSE MUTASE
IN TRYPANOSOMA CRUZI

by

Claudia Manriquez Roman, B.S.Micr.

THESIS

Presented to the Faculty of the Graduate School of
The University of Texas at El Paso
in Partial Fulfillment
of the Requirements
for the Degree of

MASTER OF SCIENCE

Department of Biological Sciences
THE UNIVERSITY OF TEXAS AT EL PASO

May 2018

Acknowledgements

First and foremost, I would like to express my gratitude to Dr. Igor C. Almeida for his unconditional support and leadership throughout this project. It was because of you that I had the opportunity to learn novel techniques in the field of parasitology, but more importantly you made me understand the importance of our role as scientists. Thank you so much for show me what real passion and happiness for science is about, that no matter how difficult the journey can be, there's always a way out. The second person I want to thank to is Dr. Rosa Maldonado. You are the reason why I stand here today. You were first person to introduce me inside the world of research. I still remember the day I met you when I was an undergraduate student, and how excited I was to meet someone who works with parasites. You offered your unconditional guidance and support, and you never stop telling me to believe in myself. Thank you, Dr. Maldonado, for everything you have done for me. I am lucky to say that I have received the best advice and guidance from two outstanding mentors who have never stopped me from pursuing my dream of become an outstanding parasitologist one day. Again, thanking for all the scientific advice, thank you for the art and history lessons, thank you for showing a little piece of Brazil and Venezuela, and finally thank you for all the caipirinhas and delicious food!

Also, I would like to show my appreciation and unconditional love to my lab members and friends from the Bioscience Research Building, specially Eva Iniguez, Jose Orozco, Susana Portillo, Caresse-Lynn Torres, Nasim Karimi Hosseini, Johnathan Abou-fadel, Jaisel Cervantes, Chenoa Arico, Bernice Caad and current and previous members from Almeida and Maldonado's lab. Thank you for all the unforgettable moments where we laughed, we cried and learned how to move forward. It is thanks to all of you that I've grown up so much not only as scientist, but also as human being. Moreover, thank you to Veronica Escalante and Teresa Cruz-Bustos for their immense support in this project. You two ladies could run the world together! In addition, I would like to thank my thesis committee members: Dr. Katja Michael and Dr. German Rosas-Acosta for your willingness to help and provide advice in the course of my project.

Finally, I will never have enough words to describe how thankful I am to my mother Alma, my father Ricardo and my brother Ricardo Jr. Mom and Dad, thank you for working so hard for giving me the best life every child deserves. It is because of you that today I'm one more step closer to become the scientist I want to be.

Abstract

The protozoan parasite, *Trypanosoma cruzi*, is the causative agent of Chagas disease (ChD), or American trypanosomiasis, which affects 6-8 million people in Latin America. It is estimated that 2-3 million people will develop severe lifelong cardiac and/or digestive disorders. ChD has become a life threat not only to endemic regions but most recently also to nonendemic regions, including the United States, owing to extensive worldwide migration in recent years. The lack of a vaccine and the limited efficacy of the two drug treatments available make it urgent to develop novel therapies to treat such a threatening disease. UDP-Galactopyranose mutase (UGM) is a flavoenzyme that catalyzes the conversion of UDP-galactopyranose to UDP-galactofuranose, the precursor of galactofuranose (Gal_f). In *T. cruzi*, Gal_f is found on O-linked oligosaccharides of glycosylphosphatidylinositol (GPI)-anchored mucin glycoproteins and glycoinositolphospholipids (GIPLs), which are highly abundant surface molecules involved in parasite virulence (mucins) and attachment to the insect-vector (GIPLs). Gal_f is found in several pathogenic organisms but not in humans, thus making the elucidation of its biosynthetic pathway attractive for the development of more effective drugs or vaccines for ChD. The limited genetic tools available to study *T. cruzi* remains a limiting factor to generate deletion mutants. Here, we propose employing the CRISPR (clustered regularly interspaced short palindromic repeats)/Cas9 (CRISPR-associated gene 9) system to knockout *T. cruzi* UGM and identify its essentiality in parasite survival and/or virulence. To this end, we employed the Cas9/sgRNA/pTREX-n attached to a green fluorescent reporter. A donor DNA containing the tag sequence and a marker for antibiotic resistance (blasticidin) were employed to repair the double strand break by homologous recombination. After 7 weeks of transfection, we demonstrated that disruption of UGM is not essential for the survival of *T. cruzi*. These experiments will further our

understanding about *T. cruzi* UGM, thus, providing potential targets that can be considered in the future development of new drugs and/or vaccines for ChD.

Table of Contents

Acknowledgements	v
Abstract.....	vi
Table of Contents	viii
List of Tables.....	x
List of Figures	xi
Chapter I: Introduction	1
I.1 Chagas disease and its causative agent, <i>Trypanosoma cruzi</i>	1
I.2 Glycoconjugates on the surface of <i>T. cruzi</i>	7
I.3 UDP-Galactopyranose mutase (UGM) and its role in the biosynthesis of beta-galactofuranose (β Gal f) in <i>T. cruzi</i>	9
I.4 What is the current toolbox to study genetic manipulation in <i>T. cruzi</i> ?	13
I.5 CRISPR/Cas9: an adaptive and sophisticated immune system for bacteria and archaea	14
I.6 The CRISPR/Cas9 type II system as a genome editing tool for <i>T. cruzi</i>	17
Chapter II: CRISPR/Cas9-mediated genetic disruption of UDP-Galactopyranose mutase in <i>T. cruzi</i>	20
II.1 Hypothesis.....	21
II.2 Specific aim	21
II.3 Materials and Methods	22
II.3.1. <i>Trypanosoma cruzi</i> epimastigote culture.....	22
II.3.2. Generation of Molecular Constructs	22
II.3.3. Amplification of donor DNA template (Blasticidin-S deaminase cassette) used for homologous recombination repair.....	24
II.3.4 Parasite transfections and selection.....	26
II.3.5. Analysis of mutant parasites.....	26
II.3.5. Fluorescence microscopy	28
Chapter III: Results	29
III.1 Molecular constructs of CRISPR/Cas9 in <i>T. cruzi</i>	29
III.2 <i>T. cruzi</i> epimastigote kill dose assay.....	31

III.3 Amplification of donor DNA (BSD cassette) to repair double strand break made by Cas 9	32
III.4 Fluorescence microscopy of <i>T. cruzi</i> UGM-KO and PFR2-KO mutant parasites	34
III.5 Generation of <i>T. cruzi</i> UGM mutants by CRISPR/Cas9-induced homologous recombination with a selectable marker	36
Chapter IV: Discussion and future studies	38
References	41
Vita	52

List of Tables

Table 1. Primers used to generate CRISPR/Cas9 constructs.	24
Table 2. Primers to amplify donor DNA used to repair DSB in PFR2 and UGM.	25
Table 3. Primers used to verify integration of donor DNA in PFR2 and UGM.	27

List of Figures

Figure 1. Estimated number of immigrants infected with *Trypanosoma cruzi* residing in nonendemic countries. Figure taken from (1).....3

Figure 2. Life cycle of *Trypanosoma cruzi*. Infection with *T. cruzi* begins when a triatomine “kissing bug” takes a blood meal, and releases metacyclic trypomastigotes in its feces. The trypomastigotes will be introduced inside the host through the insect bite wound or mucosal membranes. Upon entry in the body, the parasites will invade nucleated cells and differentiate into non-flagellated amastigotes. The amastigotes will replicate by binary fission and, after a few replication cycles, differentiate into bloodstream trypomastigotes. These forms will rupture the cell membrane and escape to the extracellular milieu to infect surrounding cells or to reach the bloodstream, and therefrom invade other cells and tissues. A new triatomine will take a blood meal and ingest bloodstream trypomastigotes from an infected mammalian host. Shortly after, they will differentiate into epimastigotes, which will replicate in the midgut of the insect vector. Upon nutritional stress, epimastigotes detach from the midgut epithelium, travel to the hindgut, and differentiate into highly infective metacyclic trypomastigotes, which will be then excreted with the feces (3,12). Figure taken from (3).4

Figure 3. Surface glyocalyx of *Trypanosoma cruzi*. (A) The surface coat of *T. cruzi* is covered by glycoproteins of three major families (i.e., mucin, TS, and MASP) and glycolipids (GIPLs), attached to the plasma membrane via a GPI-anchor (27,29). (B) Schematic representation of a typical *T. cruzi* GPI-anchored protein. EtNP, ethanolaminephosphate; AEP, aminoethylphosphonate; Man, mannose; GlcN, glucosamine; PI, phosphatidylinositol; IPC, inositolphosphoceramide or inositolphosphorylceramide. Schematic representation by I.C. Almeida (unpublished).8

Figure 4. (A) β -Gal structure. (B) Conversion of UDP-Galp to UDP-Galf catalyzed by UGM. (C) Chemical structures of oxidized and reduced forms of the flavin cofactor. Figure A was taken from ChemSpider (<http://www.chemspider.com/Chemical-Structure.9194630.html>); figures B and C were adapted from Oppenheimer et al., 2012 and Tanner et al., 2014 (44,47).. 10

Figure 5. Schematic representation of β -galactofuranose (β -Galf) expressed in GIPLS and GPI-mucin O-glycans of *T. cruzi*. (A) Proposed structure of a GIPL with one β -Galf residue in *T. cruzi* strains CL, G, G-645, and Y. (B) Proposed structure of GIPL with two β -Galf residues in *T. cruzi* strains CL, G, G-645, and Y. (C) Structure of *T. cruzi* Dm28c GPI-mucin O-glycan covalently linked to threonine (Thr) residues. The backbone of the protein core is represented as a blue ribbon. The structural representation of the GIPLs was drawn based on Carreira et al., 1996 (40), using the Symbol Nomenclature for Glycans (SNFG) (<https://www.ncbi.nlm.nih.gov/glycans/snfg.html>). O-Glycan structures were adapted from Mendonça-Previato et al., 2013 (37), and Serrano et al., 1995 (38), using the SNFG.....11

Figure 6. Biology of CRISPR/Cas system as a defense mechanism for invading foreign elements. CRISPR/Cas mediated immunity is divided in three phases: (1) acquisition; (2)

expression (CRISPR RNA biogenesis; and (3) interference. Upon infection, foreign DNA is integrated into the CRISPR locus as a new spacer “interspaced” with identical repeats. Then, the spacer elements are transcribed and matured into CRISPR RNAs (crRNAs), which will pair with complementary protospacer sequences from invading genetic elements. Each crRNA functions in complex with a Cas9 that will direct recognition and destruction of the target element. Figure taken from (69)..... 16

Figure 7. Schematic representation of the CRISPR/Cas9 complex. The RNA-guided endonuclease Cas9 from *S. pyogenes* is directed towards the target DNA leading by a sgRNA (red), which consists of 20 nt complementary to the target sequence (protospacer). In order to cleave the target sequence, Cas9 is required to recognize a PAM sequence of 5’NGG’3 (orange) that is located downstream of the target sequence in the genomic DNA. Upon DNA cleavage, the DSB can be repaired by three mechanisms: (1) NHEJ, which leads to indel (insertions or deletions) mutations on the DNA; (2) HDR, which requires the presence of a donor DNA with homologous recombination sites flanking the region where the cleavage was done; and (3) MMEJ, in which short homologous sequences are aligned on either side of the break to repair the DSB. This results in deletions flanking sequences from the original break. Figure taken from (60)..... 18

Figure 8. Restriction map used in the CRISPR/Cas9 system for genome editing of UGM and PFR2 in *T. cruzi*. Cas9/pTREX-n (56), comes from an *S. pyogenes* Cas9 sequence with a twice-repeated sequence of the simian virus 40 nuclear localization signal and a GFP in the pTREX-n backbone. The specific sgRNA fragment of each gene was inserted through the BamHI site. This plasmid confers resistance to the antibiotic neomycin (Neo). Transfection with this vector will produce green fluorescent parasites. Figure taken from Lander et al., 2015 (56). 30

Figure 9. Kill dose curve of wild-type *T. cruzi* epimastigotes (Dm28c), with different concentrations of Bsd and 250 µg neomycin (Neo). Red line represents epimastigotes without exposure to antibiotic..... 31

Figure 10. 1%-Agarose gel showing amplification of donor DNA used to repair DSB from UGM (A) and PFR2 (B). Donor DNA is shown as a PCR product of 599 bp. (A) UGM/Bsd: lane 1, Gene Ruler DNA Ladder Mix (Thermo Fischer Scientific Inc.); lane 2, water control; lane 3, PCR product. (B) PFR2/Bsd: lane 1, Gene Ruler DNA Ladder Mix (Thermo Fischer Scientific Inc.); lane 2, water control; lane 3, blank (no sample); lane 4, PCR product. 33

Figure 11. Fluorescence microscopy of PFR2 and UGM *T. cruzi* mutant parasites controlled under the expression of CRISPR/Cas9. (A) Live images of PFR2-KO mutant parasites presenting partial flagellar detachment (arrows). (B) Single PFR2-ablated epimastigote showing detached flagella (arrow). (C) UGM-KO epimastigotes with green fluorescent protein co-localized with DAPI-stained nuclei (blue)..... 35

Figure 12. Research strategy used to generate *T. cruzi* UGM and PFR2 mutant parasite by CRISPR/Cas9-induced homologous recombination. (A) Schematic representation of the strategy used to generate *T. cruzi* UGM-KO parasites using homologous recombination to repair

the DSB caused by Cas9. A blasticidin-S-deaminase cassette was inserted to repair DNA. Primers annealing outside the homologous regions of the Bsd cassette were designed to amplify a fragment of 461 bp in the intact locus of *T. cruzi* UGM, whereas in the mutant parasite, a fragment of 666 bp was amplified after insertion of Bsd cassette. **(B)** Strategy used to generate *T. cruzi* PFR2-ablated parasites. Primers outside the homology regions of Bsd were designed to amplify a fragment of 376 bp in WT parasites and 696 bp in mutant parasites. **(C)** PCR products were obtained from a 1%-agarose gel. Lanes from left to right: 1, UGM WT; 2, UGM pTREX-n/Cas9/sgscramble RNA (negative control); 3, UGM pTREX-n/Cas9 (negative control); 4, UGM-KO; 5, water control (negative control); 6, PFR2-KO (positive control); 7, PFR2-WT.... 37

Chapter I: Introduction

I.1 Chagas disease and its causative agent, *Trypanosoma cruzi*

Chagas disease (ChD), also known as American trypanosomiasis, is a neglected tropical infectious disease caused by the hemoflagellate protozoan parasite, *Trypanosoma cruzi* (*T. cruzi*). ChD was first discovered in 1909 by the Brazilian physician Carlos Chagas. Currently, the disease affects about 6 to 8 million people in Latin America (1,2). Originally confined to the poorest and rural areas of South and Central America, ChD has crossed frontiers and became an important health problem to nonendemic countries in Europe, the Western Pacific Area, Australia, Japan, and the U.S. (**Fig. 1**). A recent increase in migratory movements from people residing in endemic countries has spread and alarm about the globalization of ChD (1). Only in the United States, an estimated 300,000 people are thought to be chronically infected. On the other hand, Spain is the country having the second number of reported cases of infected immigrants (3-6).

T. cruzi is a kinetoplastid protozoan that is normally transmitted to humans and other mammal reservoirs through the infected feces of a blood-sucking triatomine insects, popularly known as “kissing bugs”, which are the disease vectors. Infection with *T. cruzi* begins when an infected triatomine insect takes a blood meal and defecates close to the wounded area (**Fig. 2**). Metacyclic trypomastigotes, which are infective forms of the parasite, are present in the insect’s excrements and will enter the body through the bite wound or exposed oral or ocular mucosa. Inside the mammalian host, the parasites will invade different types of nucleated cells, mainly by a lysosome-mediated mechanism (7). The trypomastigotes will then escape the parasitophorous vacuole to the cytoplasm and differentiate into rounded, non-flagellated amastigote forms, which

replicate by binary fission. The amastigotes will differentiate into trypomastigotes, which upon host-cell plasma membrane rupture will be released in the extracellular milieu, eventually reaching the bloodstream. The circulating trypomastigotes will travel through the bloodstream invading different tissues and organs, starting new replicative cycles in a variety of nucleated cells (7,8). Bloodstream trypomastigotes will be available to infect triatomine vectors when they blood feed from the mammalian host. Inside the kissing bug, ingested trypomastigotes will transform into the non-infective forms of the parasite, epimastigotes, inside the vector's midgut. Then, the epimastigotes will travel to the hindgut where they will transform into infective metacyclic trypomastigotes, therefore completing the life cycle of the parasite (9). Other routes of transmission include blood transfusion, organ transplantation, congenital (mother to child at birth), and laboratory accidents (10). In addition, increasing number of outbreaks of oral transmission through contaminated foods and juices have been reported (11). If the infection is left untreated, the parasite remains for the rest of the host's life span.



Figure 1. Estimated number of immigrants infected with *Trypanosoma cruzi* residing in nonendemic countries. Figure taken from (1).

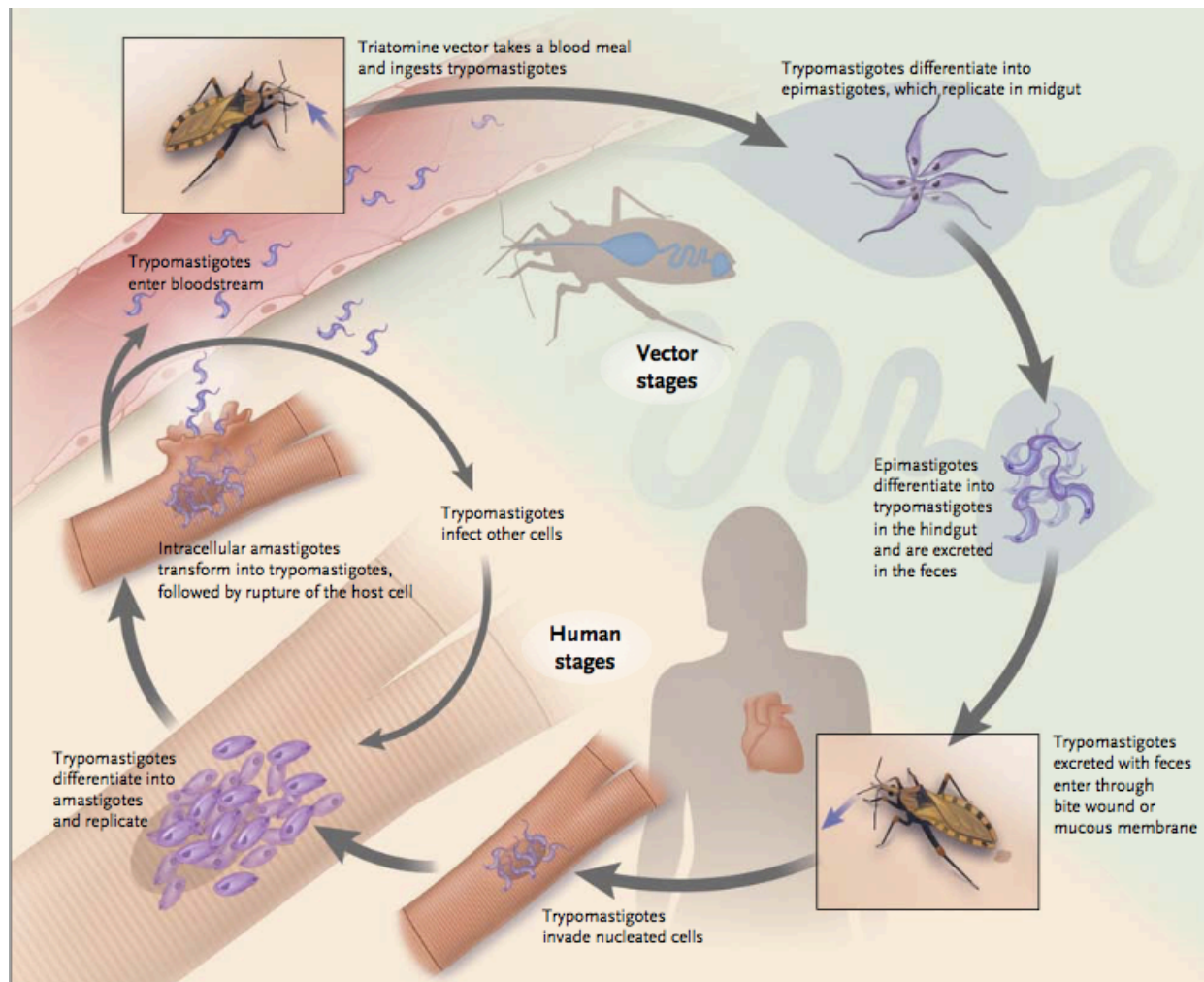


Figure 2. Life cycle of *Trypanosoma cruzi*. Infection with *T. cruzi* begins when a triatomine “kissing bug” takes a blood meal, and releases metacyclic trypomastigotes in its feces. The trypomastigotes will be introduced inside the host through the insect bite wound or mucosal membranes. Upon entry in the body, the parasites will invade nucleated cells and differentiate into non-flagellated amastigotes. The amastigotes will replicate by binary fission and, after a few replication cycles, differentiate into bloodstream trypomastigotes. These forms will rupture the cell membrane and escape to the extracellular milieu to infect surrounding cells or to reach the bloodstream, and therefrom invade other cells and tissues. A new triatomine will take a blood meal and ingest bloodstream trypomastigotes from an infected mammalian host. Shortly after, they will differentiate into epimastigotes, which will replicate in the midgut of the insect vector. Upon nutritional stress, epimastigotes detach from the midgut epithelium, travel to the hindgut, and differentiate into highly infective metacyclic trypomastigotes, which will be then excreted with the feces (3,12). Figure taken from (3).

There are three clinical phases or stages of ChD: acute, indeterminate, and chronic. The acute phase usually lasts from 4 to 8 weeks and is characterized by high parasitemia. In most of the patients, the infection is usually asymptomatic or present non-specific symptoms (e.g., general malaise, fever, fatigue, head and body aches, nausea, and vomiting). However, if the infection occurs through vector-borne transmission, the site of parasite inoculation is characterized by a skin lesion known as “Chagoma”. In other cases, inoculation occurs via the conjunctiva, which leads to periorbital swelling, palpebral edema, and conjunctivitis, which are collectively known as Romana’s sign (1,12). However, when symptoms are present, they can include fever, headache, rashes, enlarged lymph nodes, muscle pain, difficulty in breathing, and swelling. Severe acute phase, which occur in less than 1% patients, includes cases of acute myocarditis, pericardial infusion, and meningoencephalitis, which can be life-threatening if left untreated (3). Patients with low or undetectable parasitemia and no evident disease symptoms are considered to present the “indeterminate” form of the disease, which can last many years in most patients. However, approximately 30 to 40% of those asymptomatic carriers will manifest the chronic phase of the disease, which is characterized by three major clinical manifestations: cardiac, digestive, and/or cardiodigestive (1,13). During the chronic phase, ~30% of patients suffer from cardiac disorders, ranging from heart’s conduction-system abnormalities, arrhythmia, heart-muscle disorders, ventricular dysfunction, and dilated cardiomyopathy, the latest being the most serious and threatening form of ChD (10,14). A considerable number of patients in the chronic phase are under great risk of cardiac stroke, particularly anterior circulation infarction, which is one of the leading causes of death in Latin America (10,14-16). The gastrointestinal form of ChD affects the esophagus, colon, or both, resulting in megaesophagus or megacolon. Approximately 10 to 15% of chronically-ill patients will suffer from either of these medical

afflictions. Megaesophagus causes epigastric pain, regurgitation, and malnutrition in severe cases, whereas megacolon can affect the rectum or descending colon, provoking prolonged obstipation, abdominal distension, and large bowel obstruction (1).

As of today, benznidazole and nifurtimox are the only two medicines to show sufficient efficacy in the treatment of ChD. Recently, in August 2017, access to benznidazole was approved for the first time in the U.S.A., for children between 2 and 12 years, therefore moving a step forward in the treatment and recognition of tropical infectious diseases outside of endemic countries (17). If the infection is treated during the onset of the acute phase, success rate is almost 100%, and ~60-80% in children and adults with recent chronic infections. However, the chemotherapy efficacy in adults with chronic, long-established infections is significantly lower and variable (18,19). Recent clinical trials using successive quantitative PCR determinations to evaluate parasitemia, indicate that benznidazole eliminates the parasite from circulation in ~80% of patients (20,21). Similar therapeutic success has been described for nifurtimox (19). However, chemotherapy with benznidazole or nifurtimox show serious adverse effects, such as digestive intolerance, anorexia, weight loss, vomiting, headache, myalgia, among others in 10-27% of patients (3,19), therefore, outweighing the benefits from the risks in the efficacy of the treatment. In addition to the serious side effects, efficacy of these drugs usually requires a 60- and 90-day treatment regimen for benznidazole and nifurtimox, respectively, and access to these drugs are limited even in endemic countries, posing a difficult burden in the eradication of ChD. Currently, there's no clinical vaccine against ChD or any other improved therapies, despite many experimental efforts in the last several years (22-24). Consequently, it is crucial to discover new molecular targets in *T. cruzi* and develop new therapeutic approaches for ChD.

I.2 Glycoconjugates on the surface of *T. cruzi*

The surface glycocalyx of *T. cruzi* is composed of glycosylphosphatidylinositol (GPI)-anchored glycoconjugates, which are highly associated to the virulence, infectivity and survival of the parasite. These glycoconjugates include the mucin-like glycoproteins, *trans*-sialidases (TS), mucin-associated surface proteins (MASPs), and glycoinositolphospholipids (GIPLs) (**Fig. 3A**). The structure of these GPI anchors in *T. cruzi* consists of a glycan core containing four mannoses linked to a glucosamine, which is attached to a phosphatidylinositol (PI) moiety that contains one or two lipid tails. The C-terminus of the protein is linked to the glycan core via an ethanolaminephosphate (25-28) (**Fig. 3B**). The most abundant surface glycoconjugates in all morphological stages of *T. cruzi* are the mucin-like glycoproteins (or mucins) and GIPLs, which they coat approximately 60-80% of the parasite's surface (27-30). A study conducted by Pereira-Chiocola et al. (2000) demonstrated that GIPLs are more abundant in the epimastigote form of *T. cruzi*, whereas mucins outnumbered GIPLs in the trypomastigote form of the parasite (31).

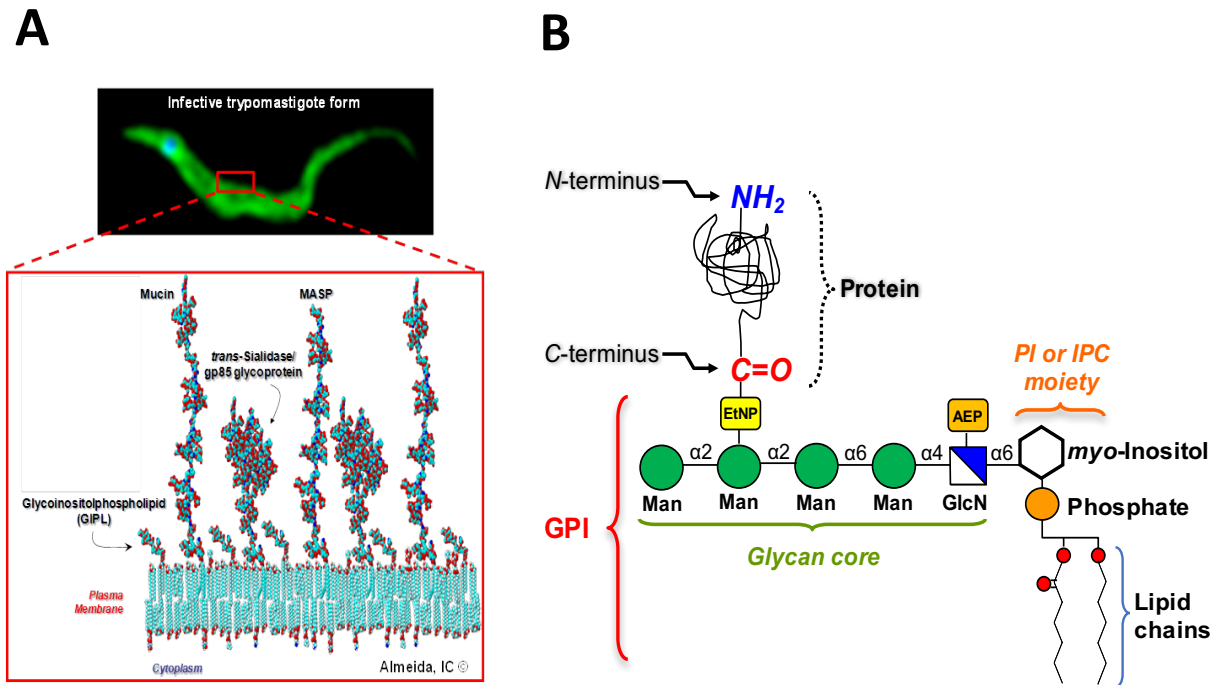


Figure 3. Surface glycocalyx of *Trypanosoma cruzi*. (A) The surface coat of *T. cruzi* is covered by glycoproteins of three major families (i.e., mucin, TS, and MASP) and glycolipids (GIPLs), attached to the plasma membrane via a GPI-anchor (27,29). (B) Schematic representation of a typical *T. cruzi* GPI-anchored protein. EtNP, ethanolaminephosphate; AEP, aminoethylphosphonate; Man, mannose; GlcN, glucosamine; PI, phosphatidylinositol; IPC, inositolphosphoceramide or inositolphosphorylceramide. Schematic representation by I.C. Almeida (unpublished).

I.3 UDP-Galactopyranose mutase (UGM) and its role in the biosynthesis of beta-galactofuranose (β Galf) in *T. cruzi*

T. cruzi possesses a dynamic life cycle, where the different sugar moieties on the cell surface are constantly changing, therefore exerting a potential role in the infectivity, cell recognition and adhesion during disease propagation, and resistance of the host's immune defense (32). Out of these molecules, there is a unique sugar present on the *T. cruzi* cell surface, known as β -galactofuranose (β -Galf) (30,32,33). β -Galf is a five-member ring form of galactose (**Figure 4A**) and it has been found on the cell surface of many other human pathogens such as *Mycobacterium tuberculosis*, *Escherichia coli*, *Salmonella typhimurium*, and *Klebsiella pneumoniae* (34). In addition, β -Galf is also present in other protozoan (trypanosomatid) parasites, such as *Leishmania major*, *L. mexicana*, *Leptomonas samueli*, *Endotrypanum schaudinni*, and *Trypanosoma dionisii* (33,35,36). In *T. cruzi*, β -Galf residues are found in O-linked oligosaccharides of glycosylphosphatidylinositol (GPI)-anchored mucins and GIPLs, playing an important role in parasite host-interactions and pathogenesis (30,32) (**Figure 5**). However, thus far, β -Galf has only been observed in O-glycans of GPI-mucins purified from strains belonging to genotype or discrete typing unit (DTU) TcI (G, Colombiana, and Dm28c) and TcVI (Tulahuen) (37,38), although the parasite has been classified into distinct six genotypes (TcI-VI) (39) (**Figure 5A**). Interestingly, β -Galf has not been found in GPI-mucin-derived O-glycans from CL-Brener strain, which like Tulahuen strain also belongs to DTU TcVI. On the other hand, β -Galf residues seem to be more ubiquitous in GIPLs, being found in every parasite genotype, strain, or clone so far analyzed (30,32,33,40) (**Figure 5B**). Different studies have shown the antigenicity of *T. cruzi* GIPLs in human and rabbit, mainly caused by the terminal β -Galf residues (30,41,42). Moreover, it was shown that GIPLs are involved in the attachment of the

parasites in the luminal midgut surface of the vector *Rhodnius prolixus* (43). The administration of 0.5 μ M Dm28c epimastigote-derived GIPLs to infected blood meal inhibited ~90% parasite attachment to the vector's midgut epithelium, demonstrating the importance of β -Gal f in the binding of *T. cruzi* epimastigotes to the insect's midgut (43).

The key enzyme responsible in the biosynthesis of β -Gal f is **uridine diphosphate (UDP)-galactopyranose mutase (UGM)**, a flavoenzyme that catalyzes the conversion of UDP-galactopyranose (UDP-Galp) to UDP-galactofuranose (UDP-Galf), the nucleotide-sugar donor of Gal f (**Fig. 4B**) (44). This enzyme was discovered for the first time in the *E. coli* K-12 strain in 1996, and later on in other pathogens such as *M. tuberculosis*, *Aspergillus fumigatus*, and *L. major*, and it was found that it was the only source to produce β -Gal f , and more importantly, that this sugar is not present in mammals (42,45,46).

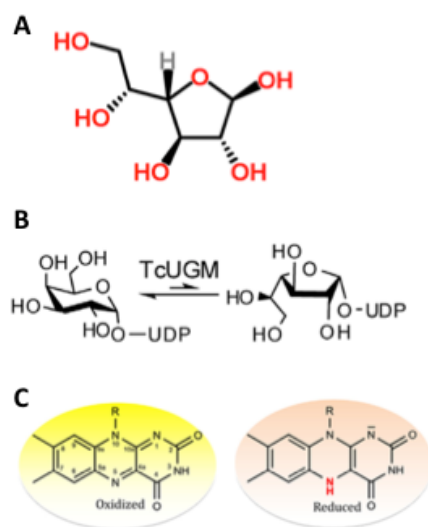


Figure 4. (A) β -Gal f structure. (B) Conversion of UDP-Galp to UDP-Galf catalyzed by UGM. (C) Chemical structures of oxidized and reduced forms of the flavin cofactor. Figure A was taken from ChemSpider (<http://www.chemspider.com/Chemical-Structure.9194630.html>); figures B and C were adapted from Oppenheimer et al., 2012 and Tanner et al., 2014 (44,47).

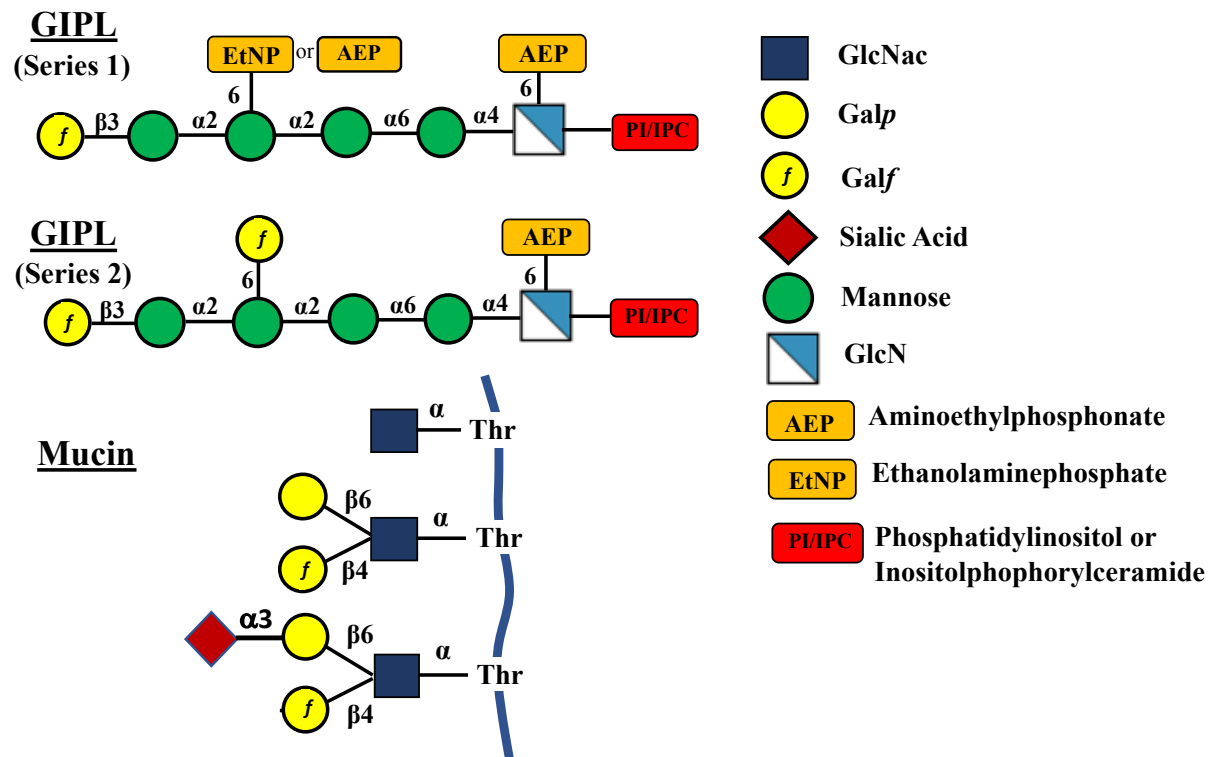


Figure 5. Schematic representation of β -galactofuranose (β -Gal f) expressed in GIPLS and GPI-mucin *O*-glycans of *T. cruzi*. (A) Proposed structure of a GIPL with one β -Gal f residue in *T. cruzi* strains CL, G, G-645, and Y. (B) Proposed structure of GIPL with two β -Gal f residues in *T. cruzi* strains CL, G, G-645, and Y. (C) Structure of *T. cruzi* Dm28c GPI-mucin *O*-glycan covalently linked to threonine (Thr) residues. The backbone of the protein core is represented as a blue ribbon. The structural representation of the GIPLs was drawn based on Carreira et al., 1996 (40), using the Symbol Nomenclature for Glycans (SNFG) (<https://www.ncbi.nlm.nih.gov/glycans/snfg.html>). *O*-Glycan structures were adapted from Mendonça-Previato et al., 2013 (37), and Serrano et al., 1995 (38), using the SNFG. Heading 8,h8 format.

In order to catalyze a non-redox reaction for the conversion of Gal p to Gal f , UGM requires the flavin cofactor to be in its reduced form (**Fig. 4C**). Different mechanistic studies of prokaryotic UGM have led to propose two different mechanisms for the ring contraction of UDP-Gal p to UDP-Gal f . The first one portrays a nucleophilic attack by the reduced flavin to form a flavin-Gal adduct. This reaction can occur in a Sn1, in which the flavin covalent intermediate is formed by the attack of N5-flavin adenine dinucleotide (N5_{FAD}) to an oxocarbenium galactose intermediated, or Sn2 manner, where the covalent flavin intermediate could be formed by the direct attach of the flavin by carbon 1 in galactopyranose (C1_{Gal p}) (44). The second proposed mechanism involves the transfer of a single electron from reduced flavin to Gal, forming a sugar-flavin adduct (44). Molecular studies have been conducted in order to demonstrate the importance of UGM in terms of virulence and survival in other pathogens. For example, deletion of genes encoding UGM in *M. tuberculosis* have shown that this enzyme is essential for the growth and survival of these bacteria (48), whereas in the fungi *A. fumigatus*, when UGM virulence was attenuated, and the fungi became more sensitive to changes in temperature and its cell wall became thinner (49,50). Moreover, when UGM was deleted from *L. major*, β Gal f was completely depleted, and the parasite expressed truncated GPIs in its membrane and was less virulent (51). Only very few studies have been conducted in order to understand the structure and chemical mechanism of this enzyme, and so far, we know that UGM catalyzes a non-redox reaction and that the flavin cofactor possess a unique role in this catalysis. Moreover, we know through the literature that UGM is important for the virulence of the parasite, however, up to date, there haven't been any studies to demonstrate what is the exact role this enzyme plays in the pathogenesis of *T. cruzi*, and would happened in the absence of it (44,47,52). **As previously mentioned, it is well established that this enzyme is not present in**

humans (47), thus making the elucidation of its biosynthetic pathway attractive for the development of potential drug targets or vaccines to treat Chagas disease.

I.4 What is the current toolbox to study genetic manipulation in *T. cruzi*?

The available chemotherapy to treat ChD has proven to be very unsatisfactory due to its lack of full efficacy in the chronic phase and its various severe side effects. In addition, there are no vaccines to prevent or treat the disease. Therefore, it is imperative to use new molecular approaches to study the biology of *T. cruzi* in order to develop new or better therapeutic options.

With the advent of the full genomic sequence of *T. cruzi* in 2005, major breakthroughs in genome-based studies have allowed us to understand the function of molecular factors that are essential for the pathogenesis caused by this parasite, leading to the development of new diagnostic tools and better therapeutic options. At the same time, new molecular approaches have been created to assess and characterize gene function in *T. cruzi* in its different morphological stages and how it affects its host. Some of them include gene deletion, overexpression, insertion of reporter genes and subcellular localization of proteins. Moreover, reverse genetics approaches, such as the development of stable tetracycline-regulated expression vectors or high throughput cloning systems based on Gateway technology, have greatly benefited large-scale genome projects in trypanosomes (53-55). However, the availability of genetic and molecular tools to study *T. cruzi* is still limited (56,57). As of today, the pTREX vector plasmid has proven to be the best genetic tool available in the expression and functional analysis of *T. cruzi* genes. This system is driven by a ribosomal promoter that improves gene integration, expression and clonal selection (58). However, genetic editing in *T. cruzi* is still very behind in comparison to other kinetoplastid parasites such as *Trypanosoma brucei*, where the RNA

interference technique has been well established. Moreover, *T. cruzi* requires approximately 6-8 week to generate clone mutant epimastigotes (4 times higher than *Leishmania* epimastigotes and 8 times longer than *T. brucei* bloodstream trypomastigotes) and the rounded-shape amastigotes require a host cell to proliferate. In addition, laboratory accidents with virulent strains makes very challenging the construction of molecular models in *T. cruzi* (56,57,59).

I.5 CRISPR/Cas9: an adaptive and sophisticated immune system for bacteria and archaea

In recent years, the field of genomic editing has been revolutionized by the emergence of a novel technique called CRISPR/Cas9 (Clustered regularly interspaced short palindromic repeats)/(CRISPR-associated gene 9), and RNA-guided system that has been applied all around the world in the genetic manipulation of all type of organisms, such as yeast, mammalian cells and protozoan parasites (60,61). Initially discovered more than 20 years ago, the CRISPR system was first described in *E. coli* when a group of scientists found an array of short repetitive sequences interspaced with non-repetitive sequences (62). Later on, they observed that these repetitive arrays were found in numerous bacteria and archaea and the spacers were identical to mobile genetic elements (bacteriophage DNA, plasmids, etc.). Alongside, they also found that these arrays were often associated with a set of Cas genes, encoding for potential helicases, nucleases and various RNA-binding proteins based on sequence similarity(61,63). Over the years, investigators concluded that these CRISPR systems are indeed adaptive defense systems that protect bacteria and archaea from invading viruses and plasmids. The CRISPR/Cas defense system is mediated via a three-step process: acquisition/adaptation, expression and interference. The acquisition step begins when viral DNA gets into the cell and the foreign DNA is detected. Here, the CRISPR system allows for integration of these short pieces of DNA in the CRISPR

locus by employing several of these Cas proteins. Subsequently the CRISPR sequences are transcribed into short pieces of CRISPR RNA (crRNA). These are then used with proteins encoded by these Cas genes and work together by forming interfering complexes. They employ information from RNA to base pair with the matching sequence in viral DNA and cut it (64-66). Overall, there are three types of CRISPR/Cas systems, from which type I and III present similar features, such as a large complex of specialized Cas proteins for crRNA guiding and recognition. In contrast, type II system relies on a single Cas protein, Cas9, for RNA-guided DNA recognition and cleavage of foreign DNA (61,67) (**Fig. 6**). However, a recent study conducted in 2011 by Makarova et al., which involved extensive analysis of genomic data, demonstrated evidence for two new putative types in the CRISPR/Cas system, type IV and type V (68). With this process, bacteria and archaea are allowed to eliminate foreign DNA elements in a memory-based system.

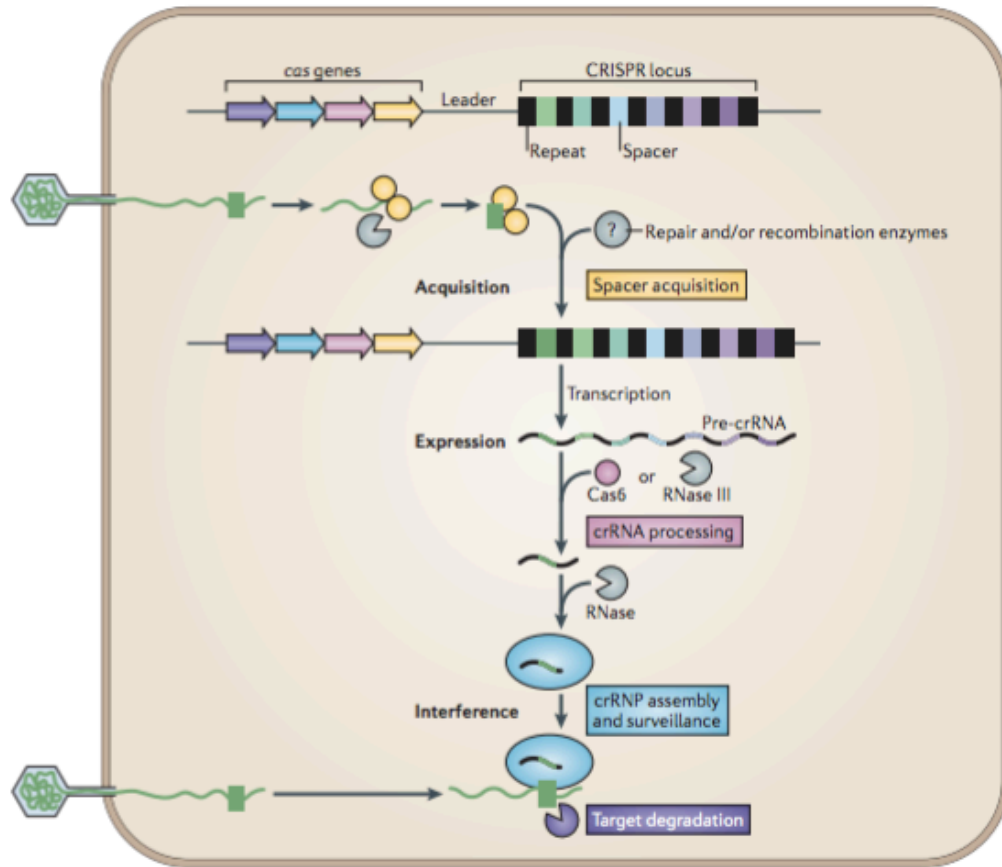


Figure 6. Biology of CRISPR/Cas system as a defense mechanism for invading foreign elements. CRISPR/Cas mediated immunity is divided in three phases: (1) acquisition; (2) expression (CRISPR RNA biogenesis); and (3) interference. Upon infection, foreign DNA is integrated into the CRISPR locus as a new spacer “interspaced” with identical repeats. Then, the spacer elements are transcribed and matured into CRISPR RNAs (crRNAs), which will pair with complementary protospacer sequences from invading genetic elements. Each crRNA functions in complex with a Cas9 that will direct recognition and destruction of the target element. Figure taken from (69).

I.6 The CRISPR/Cas9 type II system as a genome editing tool for *T. cruzi*

The CRISPR/Cas9 type II system was adapted for genome engineering from *Streptococcus pyogenes* and has been remodeled in different human pathogens such as *Toxoplasma gondii*, *Plasmodium falciparum*, *Leishmania* spp., *Cryptosporidium parvum*, and *T. cruzi* (60). Out of the three systems, this is the simplest one, as it only requires two main components, a Cas9 endonuclease and crRNA chimera, known as guide RNA, that uses RNA for target site recognition (61). This duplex, called single-guide RNA (sgRNA), is formed by the fusion of a crRNA that pairs with complementary sequences of target DNA, and a trans-activating crRNA (tracrRNA) which facilitates the maturation and processing of the crRNA. This sgRNA consists 20 nucleotides (nt) that will direct the Cas 9 to the specific target sequence using RNA-DNA base-pairing complementary rules. The sgRNA pairs with the DNA target (known as protospacer) upstream of a protospacer-adjacent motif (PAM), with the canonical form of 5' NGG (where N is any nt, and G is guanine), thus directing Cas9 to target site and produce double strand breaks (DSB) (66,70). Cas9-induced DSB can be repaired by NHEJ (non-homologous end joining), which is error prone and leaves scars in the form of insertion/deletion(indel) mutations, HDR (homology directed repair), which occurs in the presence of a donor DNA, and the DSB is repaired through homologous recombination or MMEJ (microhomology-mediated end joining), in which microhomology regions aligned on either side of the strand break, are aligned together, causing deletion of genes between these two homology sites (**Fig. 7**). It is important to highlight that even though other molecular tools, such as ZFN and TALENS, exist to produce DSB, they rely on protein-based DNA recognition, which requires a lot of protein engineering. In contrast, CRISPR/Cas9 relies on simple base-pair rules

between RNA and the target DNA, and the system can be easily modified by changing to change its target by simply editing a protospacer in the gRNA (61,66,67,71).

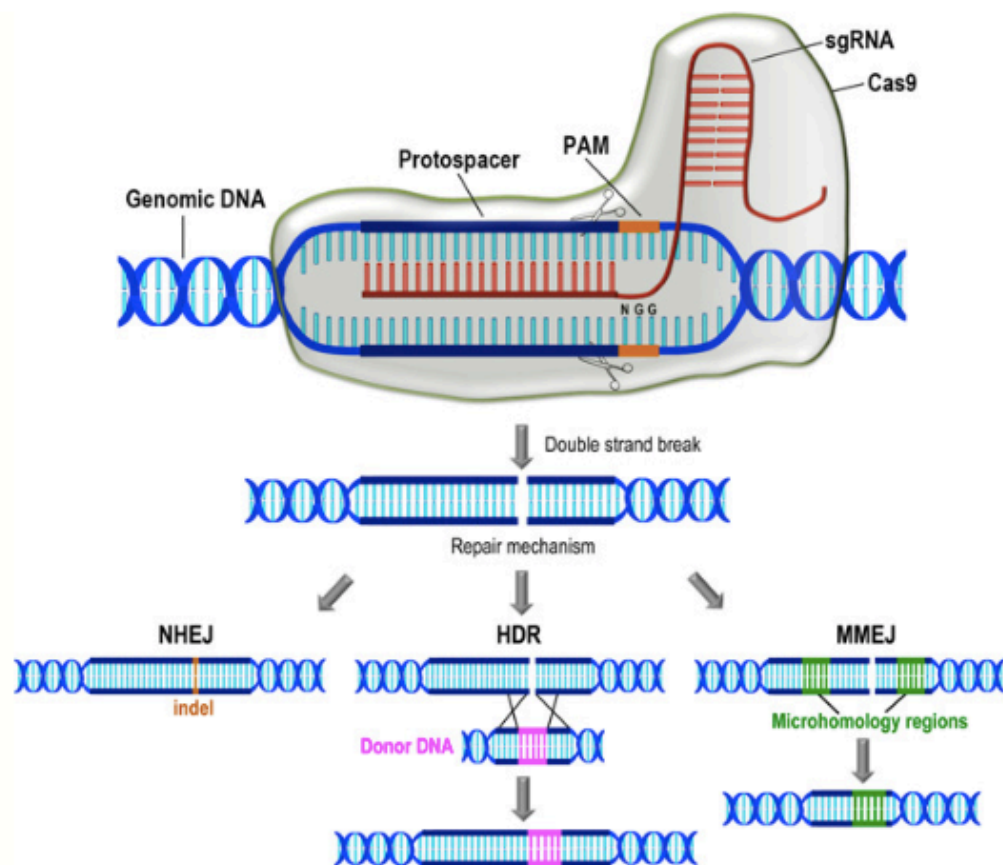


Figure 7. Schematic representation of the CRISPR/Cas9 complex. The RNA-guided endonuclease Cas9 from *S. pyogenes* is directed towards the target DNA leading by a sgRNA (red), which consists of 20 nt complementary to the target sequence (protospacer). In order to cleave the target sequence, Cas9 is required to recognize a PAM sequence of 5'NGG'3 (orange) that is located downstream of the target sequence in the genomic DNA. Upon DNA cleavage, the DSB can be repaired by three mechanisms: (1) NHEJ, which leads to indel (insertions or deletions) mutations on the DNA; (2) HDR, which requires the presence of a donor DNA with homologous recombination sites flanking the region where the cleavage was done; and (3) MMEJ, in which short homologous sequences are aligned on either side of the break to repair the DSB. This results in deletions flanking sequences from the original break. Figure taken from (60).

The first study using the CRISPR/Cas9 system as a genome editing tool for *T. cruzi* was reported by Peng et al. (2014) demonstrated a rapid and efficient tool to knockout multiple endogenous genes. Here, they generated mutant cell lines that constitutively expressed Cas9 and delivered a sgRNA by electroporation without donor DNA, demonstrating by genome-sequencing that *T. cruzi* DNA repair, in the absence of a donor DNA, can be carried out by microhomology-mediated end joining (MMEJ). More importantly, their work demonstrated that the CRISPR/Cas9 system can be used to knockout multiple genes in a large gene family of genes (β -galactofuranosyl glycosyltransferase (β -GalGT) family of 65 annotated genes), therefore opening the door to use CRISPR/Cas-mediated knockout libraries in conserved gene families (72).

A year later, another research group led by Dr. Roberto Docampo at the University of Georgia-Athens, reported the usage of CRISPR/ Cas9 system to disrupt the endogenous genes paraflagellar rod protein 1 (PFR1), paraflagellar rod protein 2 (PFR2) and GP72, a glycoprotein localized between the flagellum and the cell body. PFR1 and PFR2 are core components of the parasite's flagellum. Herein, the silenced these genes by using pTREX vectors containing Cas9 and sgRNA together or separately, or a vector containing sgRNA and Cas9 plus a donor DNA (to repair DSB by homologous recombination). Results showed successful genome silencing of PFR2, PFR2 and GP72 with undetectable toxicity of Cas9 (56). Right after this, they were able to use their established CRISPR/ Cas 9 system to endogenously tag *T. cruzi* proteins (73). In summary, achievement of genome editing in *T. cruzi* using CRISPR/Cas9 has greatly improved our understating and manipulation at the level of DNA in this parasite, leading to new strategies that could potentially lead to development of a vaccine or new chemotherapeutic treatment.

Chapter II: CRISPR/Cas9-mediated genetic disruption of UDP-Galactopyranose mutase in *T. cruzi*

The complex surface coat of *T. cruzi* is composed of GPI-anchored glycoconjugates which are highly associated to the virulence, survival and infectivity of the parasite. These glycoconjugates include the GPI-mucins, *trans*-sialidases (TSs), mucin-associated surface proteins (MASPs) and glycoinositolphospholipids (GIPLs). They most abundant glycoconjugates in the *T. cruzi* are the heavily glycosylated mucin-like molecules and the phospholipids GIPLs. It is known from previous studies, that GIPLs are more abundant in the epimastigote form of the parasite, whereas GPI-mucins are more abundant in the infective form the parasite, which is the trypomastigote form. The sugar β Galf is present in both glycoconjugates and could be a virulence factor for the parasite, like in *L. major* (51). More importantly, β Galf is not present in humans, therefore is considered an ideal drug target (25,31,42).

The **main objective** of our project is to eliminate UGM, the sole enzyme responsible for the synthesis of β Galf, from *T. cruzi*, using the CRISPR/Cas9 approach and identify its essentiality for the parasite. To this end, we will use epimastigote of the Dm28c strain as it has been demonstrated that this sugar is present in this strain (42).

II.1 Hypothesis

We hypothesize that UGM is not essential for the survival of *T. cruzi*, but it might be important for the virulence of *T. cruzi*.

II.2 Specific aim

To knockout UDP-galactopyranose mutase (UGM) in *T. cruzi* using the CRISPR-Cas9 system.

II.3 Materials and Methods

II.3.1. *Trypanosoma cruzi* epimastigote culture

T. cruzi epimastigotes (Dm28c clone) were grown in liver infusion tryptose (LIT) medium supplemented with 10% heat inactivated fetal bovine serum (iFBS) at 27°C (74). CRISPR mutant cell lines were maintained in medium containing 200 µg/ml blasticidin and/or 250 µg/ml neomycin. Growth of epimastigotes will be determined by measuring a change in optical density from the starting concentration. A kill dose assay was conducted in order to determine the minimum inhibitory concentration (MIC) for the antibiotics used for selection, blasticidin (bsd) and neomycin (neo). Previously, the MIC for neomycin had been found to be 250 µg/mL (56). The MIC for blasticidin, in the presence of neomycin was determined by measuring parasite viability over time by varying the concentration of blasticidin, namely from 350-50 µg/mL. We determined the amount of parasite by counting cells in a Cellometer X2 (Nexcelom Bioscience) counting chamber for 15 days. Results were graphed using GraphPad Prism 6.

II.3.2. Generation of Molecular Constructs

The genomic DNA sequences of the targeted gene UGM (TriTrypDB accession number TCDM_02308; http://tritrypdb.org/tritrypdb/app/record/gene/TCDM_02308) and PFR2(TriTrypDB accession number TcCLB.511215.119); <http://tritrypdb.org/tritrypdb/app/record/gene/TcCLB.511215.119>). were obtained from the

TriTrypDB database. Since PFR2 has been previously knocked out by this system, we decided to employ it as a positive control. All the molecular constructs were kindly provided by Dr. Roberto Docampo (University of Athens- Georgia) Protospacer and small-guide RNAs (sgRNA) specific for UGM and PFR2 were designed and PCR amplified following the protocol established by the Docampo lab (56). The detailed protocol is available at <http://www.bio-protocol.org/e2299>. In short, the protospacer is a small sequence (~20 nt) that dictates where the gene will be cut. Here, we decided to cut in the first 100-200 bp from the start site. In order to verify that the selected protospacer did not generate off-targeting cut sites on the genome, we employed the Eukaryotic Pathogen CRISPR guide RNA/DNA Design Tool (<http://grna.ctegd.uga.edu/>) (75) and the software ProtoMatch v1(56). sgRNAs for UGM and PFR2 were amplified by PCR with their specific forward primers and a common reverse primer and cloned into pUC_sgRNA (vector) (**Table 1**). These PCR products were subsequently cloned into the pCR2.1-TOPO vector (Invitrogen Life Technologies) and several clones sent for sequencing with universal primers for the T7 promoter to confirm the sequence as well as its orientation. Following, the protospacers were cut out from the pCR2.1-TOPO vectors and cloned into the Cas9/pTREX-n vector (Addgene) by using the BamHI site. Transformations were performed using the *E. coli* DH5 α strain (New England Biolabs) and clones selected with neomycin. Recombinant clones were picked and analyzed by PCR and subsequently sequenced to confirm the orientation of the insert. These clones will correspond to the constructs pTREX/sgRNA/Cas9/UGM and pTREX/sgRNA/Cas9/PFR2 (56). Positive clones were isolated to obtain 100 μ g of plasmid DNA by Maxiprep (Qiagen) to perform at least 3 transfections. Following the Maxiprep procedure, plasmid DNA was precipitated by adding 2.5 volumes of 100% ethanol (EtOH) and 0.1 vol. of 3 M sodium acetate pH 5.2. The mixture was stored at -20°C overnight (ON). The sample was then

centrifuged at 16,000 g in a microcentrifuge (Model 5415R, Eppendorf) for 12 min, at 4°C, and the pellet carefully resuspended in 70% EtOH. Again, the mixture was centrifuged at max. speed for 3 min, and the pellet air-dried. The dried pellet was resuspended in 20 µL nuclease-free water (73).

Table 1. Primers used to generate CRISPR/Cas9 constructs.

Primer	Sequence
sgRNA-PFR2 Fw	5'GATCGGATCCGGCACC GCCGGCTGCTGCTGGTCCGGTT TTAGAGCTAGAAATAGC3'
sgRNA-UGM Fw	GATCGGATCCGAGTGTAACGACACCCCAGGGTTTTAGAG CTAGAA ATAGC
Common Reverse Primer	5'-CAGTGGATCCAAAAAAGCACCGACTCGGTG-3'.

II.3.3. Amplification of donor DNA template (Blasticidin-S deaminase cassette) used for homologous recombination repair

Ultramers for UGM and PFR2 were designed to amplify a DNA cassette that will induce DNA repair by homologous recombination containing a selectable marker blasticidin-S deaminase (Bsd) using the pCRr2.1 TOPO vector (kindly provided by Docampo's lab at UGA) as a template (56) for homologous recombination. The PCR protocol was modified from Lander et al., 2015 (56) where 50 µL final volume were used containing 25 µL GoTaq® Green Master Mix 2X (Promega), 1µL ultramer PFR2-BSD-Fw and 1µL ultramers PFR2-BSD-Rv (**Table 2**), 1 µL Template DNA (TOPO/Bsd/PFR2) and 22 µL nuclease-free water. Thermocycler conditions begin with an initial denaturation of 98° for 30 sec, followed by 35 cycles of 98°C for 15 sec, 45°C for 30 sec, and 72°C for 30 sec. A final extension was carried at 72°C for 5 min. In

order to amplify the donor DNA for UGM, we used 0.5 μ L Phusion® DNA Polymerase (NEB), 10 μ L GC Buffer, 1 μ L 10mM dNTPs, 1 μ L template DNA, 2.5 μ L reverse ultramer and 2.5 μ L forward ultramer (**Table 2**), and 1.5 μ L sterile DMSO. The reaction was completed to final volume of 50 μ L nuclease free water. Several PCR reactions (1000 μ L) were performed to obtain 50 μ g of donor DNA. The amplified sequence (599 bp) was analyzed by gel electrophoresis in a 2% agarose gel stained with 1 μ L ethidium bromide (56) PCR Products were purified using a PCR purification kit from Qiagen (Valencia, CA). Thereafter, DNA concentration was measured, and the donor DNA was precipitated by adding 2.5 volumes of 100% ethanol (EtOH) and 0.1 vol. of 3M sodium acetate pH 5.2. The mixture was stored at -20°C overnight (ON). The donor DNA was then centrifuged at 16,000 g, at 4°C, in a microcentrifuge (Model 5415R, Eppendorf) for 12 min, and the pellet carefully resuspended in 70% EtOH. Again, the mixture was centrifuged at max. speed for 3 min, and the pellet air-dried. The dried pellet was resuspended in 20 μ L nuclease-free water (73).

Table 2. Primers to amplify donor DNA used to repair DSB in PFR2 and UGM.

Primer	Sequence
PFR2-BSD-Fw (ultramer)	5'CCTTTACACAGACTCTACAAAGATACCAAATCTCACACCAGG AAAAAAAAAAGGAAATAACAACAAAAACAAACAAGGAAAC AAACAACCAAACA AGCAATGGCCAAGCCTTTGTCTCA-3'
PFR2-BSD-Rv (ultramer)	5'CGTCTCGCTCCAGTCCGACACGTGCAGGTCCTGGATGAACTC CTCGTTCGACAGGCAGGAGGTCTTCAGCTTCAGGTTGTGGATC TTCTGCTTGCGCGCATTAGCCCTCCCACACATAAC-3'
UGM-Bsd-Fw (ultramer)	5'CATACTCTTGCGGGCAACACCGACAGCAAAGCACGACCAC AAATCCTTAACCTCCGGCAATAAACTGAGGAACATCTATAAA AATATTTTATTACTAATGGCCAAGCCTTTGTCTCA-3'
UGM-Bsd-Rv (ultramer)	5'CACCCACCGCCCCCGCACCCAAACCCACGATTCTCGCTGCAG CACGTTCCAACCCTGCACTGCCCAATCCATCACATCATCAAAG TATTGATAATGCGAATTAGCCCTCCCACACATAAC-3'

II.3.4 Parasite transfections and selection

T. cruzi Dm28c clone epimastigotes (4×10^7 cells, at room temperature [RT], suspended in phosphate-buffered saline [PBS], pH 7.4) were transfected in ice-cold CytoMix (25 mM HEPES, 120 mM KCl, 0.15 mM CaCl_2 , 10 mM K_2HPO_4 , 2 mM EGTA, 5 mM MgCl_2 , 0.5% glucose, 100 $\mu\text{g/ml}$ bovine serum albumin [BSA], 1 mM hypoxanthine [pH 7.6]) containing 50 μg of each plasmid construct (pTREX-n/Cas9/sgRNA UGM, pTREX-n/Cas9/sgRNA PFR2) and donor DNA in 4-mm electroporation cuvettes with three pulses (1500 V, 25 μF) delivered by a Gene Pulser II (Bio-Rad). In addition, the following controls were included: pTREX-n/Cas9, pTREX-n/Cas9/sgscramble RNA, WT epimastigotes transfected with water, and WT epimastigotes electroporated alone. Each transfection was performed in triplicates. After the electroporation, each cuvette was placed at room temperature (RT) for 15 min. Thereafter, the parasites were electroporated parasites were transferred to a flask containing 5mL of LIT media supplemented with 20% iFBS and incubated at 27°C. After 24 h, antibiotics for selection were added. For mutant parasites that were co-transfected with the pTREX-n/Cas9/sgRNA vector and donor DNA (blasticidin cassette), their double-resistant selection was maintained in medium containing 250 $\mu\text{g/ml}$ Neomycin (Thermo Fisher Scientific) and 200 $\mu\text{g/ml}$ Blasticidin (Gibco) until stable cell lines were obtained. The controls were maintained in medium containing only 250 $\mu\text{g/ml}$ Neomycin. For a period of 7 weeks, media supplemented with 20% iFBS and fresh antibiotics were replaced every week.

II.3.5. Analysis of mutant parasites

After 7 weeks of the transfections, gDNA from mutant parasites maintained under drug selection was extracted. Briefly, 1 mL of parasite culture was centrifuged for 10 min at 800 g, at 4°C. Thereafter, the parasite pellet was resuspended in 150µL of TELT (50 mM Tris pH 8, 62.5 mM EDTA pH 8, 2.5 M LiCl, 4% Trion X-100) buffer by inverting the tube three times and then incubated for 5 min at RT. Then, 150µL of Phenol: Chloroform: Isoamyl Alcohol (25:24:1, v/v) (Thermo Fischer Scientific) was added and incubated for 5 min in a shaking rocker. The mixture was centrifuged at 16,000 g, for 5 min at 4°C and the aqueous phase was collected. The gDNA was precipitated following the protocol described by Lander et al., (2016) (73). Disruption of *T. cruzi* UGM and PFR2 (positive control) was verified by PCR analysis with primers (**Table 3**) annealing outside the homologous regions of the donor DNA (Bsd cassette). For both genes we used the Phusion High-Fidelity DNA Polymerase (New England Biolabs). A 50 µL final volume were used containing 0.5 µL of Phusion DNA Polymerase, 10 µL 5X Phusion HF buffer, 1 µL dNTPs (10mM), 1 µL forward primer, 1 µL reverse primer, 1 µL DMSO and 1 µL gDNA (100ng/ µL). Thermocycler conditions begin with an initial denaturation of 98° for 30 sec, followed by 35 cycles of 98°C for 10 sec, 60°C for 30 sec, and 72°C for 20 sec. A final extension was carried at 72°C for 10 min. The amplified sequence for UGM-KO, PFR2-KO and respective controls were analyzed by gel electrophoresis in a 2% agarose gel stained with 1µL ethidium bromide.

Table 3. Primers used to verify integration of donor DNA in PFR2 and UGM.

Primer	Sequence
PFR2-Fw-disruption verification	5'-CACATAATACTCATTCATGCAAAAC-3'
PFR2-Rv-disruption verification	5'-AAGTTCTTGCGCCTTCTCGT-3'
UGM-Fw-disruption	5'-CTCATAGCTGGTCTTGCAAC-3'

verification	
UGM-Rv-disruption verification	5'-GTTCCGGCAAACGATGAA-3'

II.3.5. Fluorescence microscopy

Transfected epimastigotes at a density of 1×10^6 cells were harvested by centrifugation at 800 g, for 10 min, at 4°C. Parasite pellet was washed with PBS, and allowed to settle in poly-L-lysine coated microscope slides (Thermo Fisher Scientific) for 10 min. Then, the parasites were fixed with 4% paraformaldehyde (Thermo Fisher Scientific) for ten minutes, washed one more time with PBS and mounted with anti-fade mounting medium with DAPI (4',6-diamidino-2-phenylindole, dihydrochloride, Vector Laboratories, Inc.) (76). Microscope slides were observed with a (Zeiss LSM 700 Laser Scanning Microscope).

Chapter III: Results

III.1 Molecular constructs of CRISPR/Cas9 in *T. cruzi*

The sequences of UGM and PFR2 were obtained from the TriTrypDB database. Once the protospacers and sgRNAs were designed, they were cloned into the pTREX-n vector. The pTREX-n vector contains the Cas9-HA-2XNLS-GFP fusion gene, which consists of the *S. pyogenes* Cas9 sequence with a simian virus (SV40) nuclear localization signal (2XNLS) repeated twice and a GFP (green fluorescence protein) marker. Here, Neomycin was added as a selectable marker to confer resistance in mutant parasites. The sequence of our sgRNA for each gene and Cas9 was added upstream and downstream of the HX1 trans-splicing signal in the pTREX-n vector(56) As a result, we generated the *T. cruzi* PFR2 pTREX-n/Cas9/sgRNA and *T. cruzi* UGM pTREX-n/Cas9/ sgRNA vectors as shown in **Figure 8**. The full sequence map for pTREX-n/Cas9 can be obtained from Addgene plasmid (<https://www.addgene.org/68708/>).

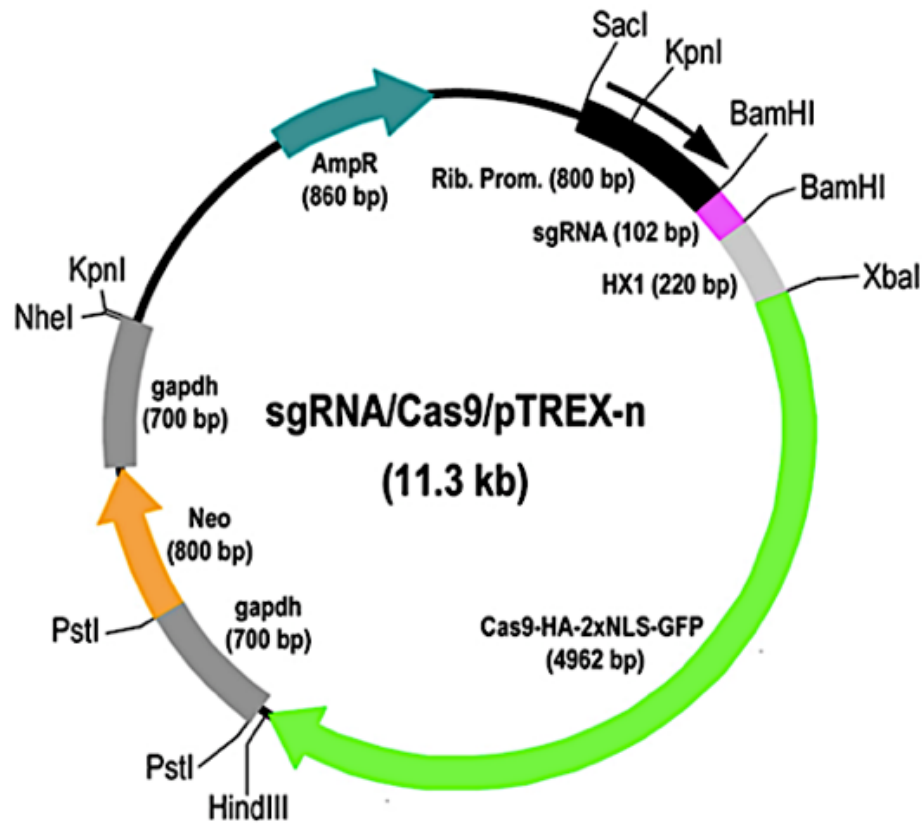


Figure 8. Restriction map used in the CRISPR/Cas9 system for genome editing of UGM and PFR2 in *T. cruzi*. Cas9/pTREX-n (56), comes from an *S. pyogenes* Cas9 sequence with a twice-repeated sequence of the simian virus 40 nuclear localization signal and a GFP in the pTREX-n backbone. The specific sgRNA fragment of each gene was inserted through the BamHI site. This plasmid confers resistance to the antibiotic neomycin (Neo). Transfection with this vector will produce green fluorescent parasites. Figure taken from Lander et al., 2015 (56).

III.2 *T. cruzi* epimastigote kill dose assay

T. cruzi epimastigotes (Dm28c clone) were grown at 28°C in liver infusion tryptose (LIT) medium supplemented with 10% FBS (74). A kill dose assay was performed in order to obtain the MIC for the 2 antibiotics used for selection, neomycin and blasticidin. For two weeks, epimastigotes were grown at different concentrations of Bsd (350-50 µg/mL) and Neo (250 µg/mL). Every day, we determinate the number of parasites by counting them in a Cellometer chamber. As observed in **Figure 9**, the different concentrations of Bsd with Neo killed the same number of parasites, in comparison to the negative control.

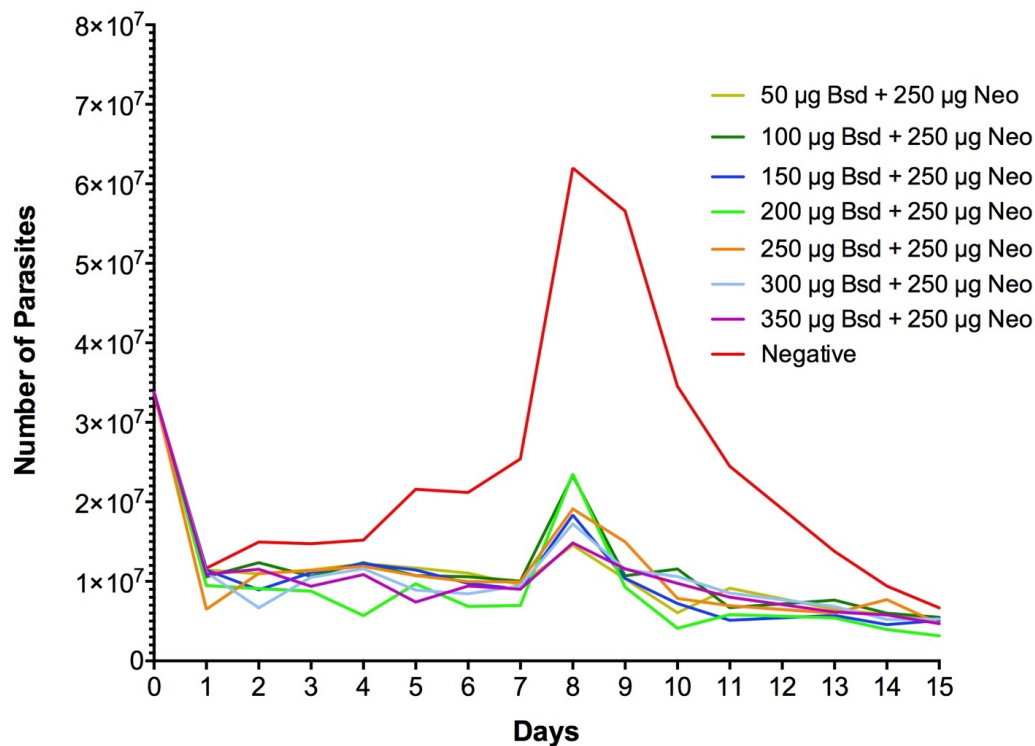


Figure 9. Kill dose curve of wild-type *T. cruzi* epimastigotes (Dm28c), with different concentrations of Bsd and 250 µg neomycin (Neo). Red line represents epimastigotes without exposure to antibiotic.

III.3 Amplification of donor DNA (BSD cassette) to repair double strand break made by Cas 9

Ultramers were designed to amplify a donor DNA cassette that will repair the DSB by homology recombination. The donor DNA amplified 100bp upstream and 100bp downstream of the Cas9 cutting site plus 399bp of the marker Blasticidin used for antibiotic resistance. Multiple PCR reactions using the Promega GoTaq® Green Master Mix and the Phusion® High-Fidelity DNA Polymerase (New England Biolabs) were used to amplify the donor DNA of PFR2 and UGM, respectively. Thereafter, the amplification of donor DNA for UGM and PFR2 were analyzed in a 1% agarose gel, showing a band corresponding of 599 bp corresponding to the donor DNA of each gene (**Figure 10**). Subsequently, the PCR reactions were purified and precipitated with ethanol to obtain 50 µg of donor DNA necessary for transfection.

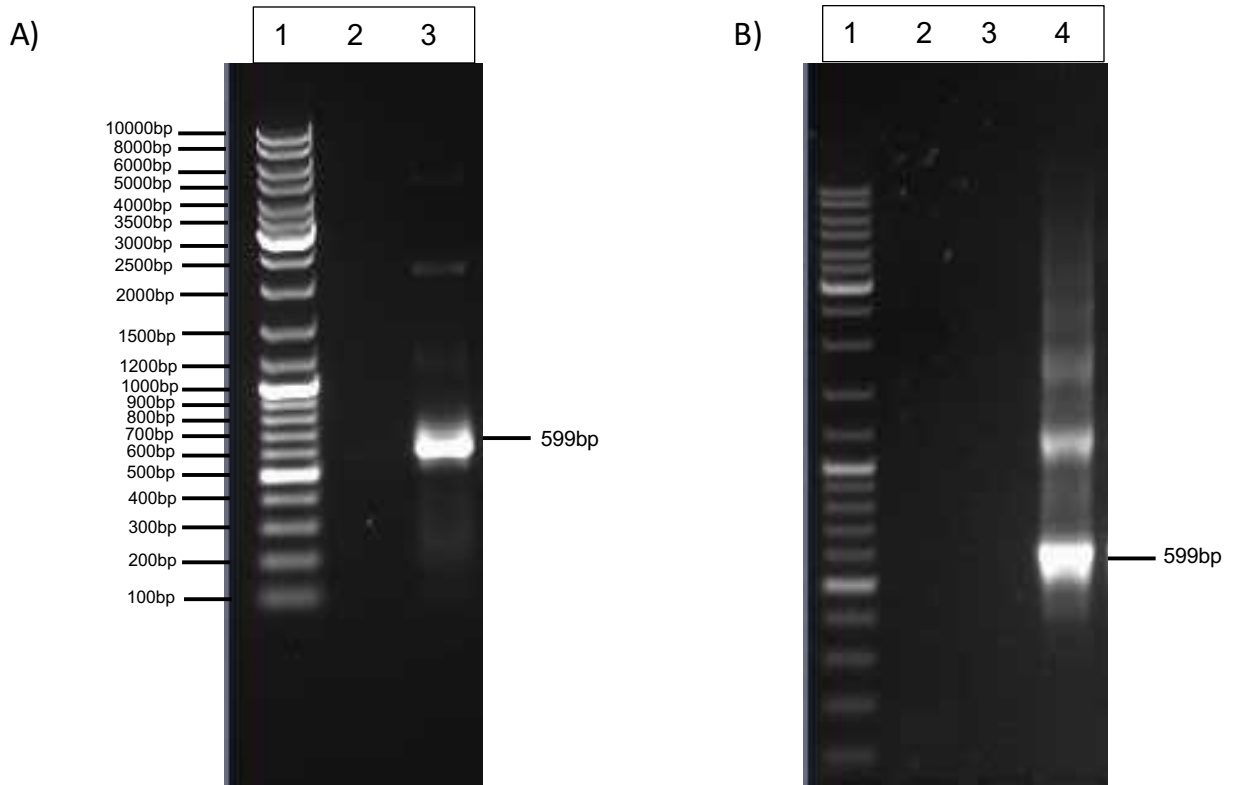


Figure 10. 1%-Agarose gel showing amplification of donor DNA used to repair DSB from UGM (A) and PFR2 (B). Donor DNA is shown as a PCR product of 599 bp. (A) UGM/Bsd: lane 1, Gene Ruler DNA Ladder Mix (Thermo Fischer Scientific Inc.); lane 2, water control; lane 3, PCR product. (B) PFR2/Bsd: lane 1, Gene Ruler DNA Ladder Mix (Thermo Fischer Scientific Inc.); lane 2, water control; lane 3, blank (no sample); lane 4, PCR product.

III.4 Fluorescence microscopy of *T. cruzi* UGM-KO and PFR2-KO mutant parasites

In our study, we used a positive control *T. cruzi* PFR2, because its genome editing produce visible changes in its phenotype, as it is an important component of the paraflagellar rod in the parasite. As observed in **Figure 11A, B**, the parasites present a certain level of flagellar detachment. In UGM-KO epimastigotes, confocal microscopy revealed that GFP fusion proteins was relocated mostly at the posterior site of the parasite (**Figure 11C**), therefore demonstrating the integration of the pTREX-n/Cas9/sgRNA vector.

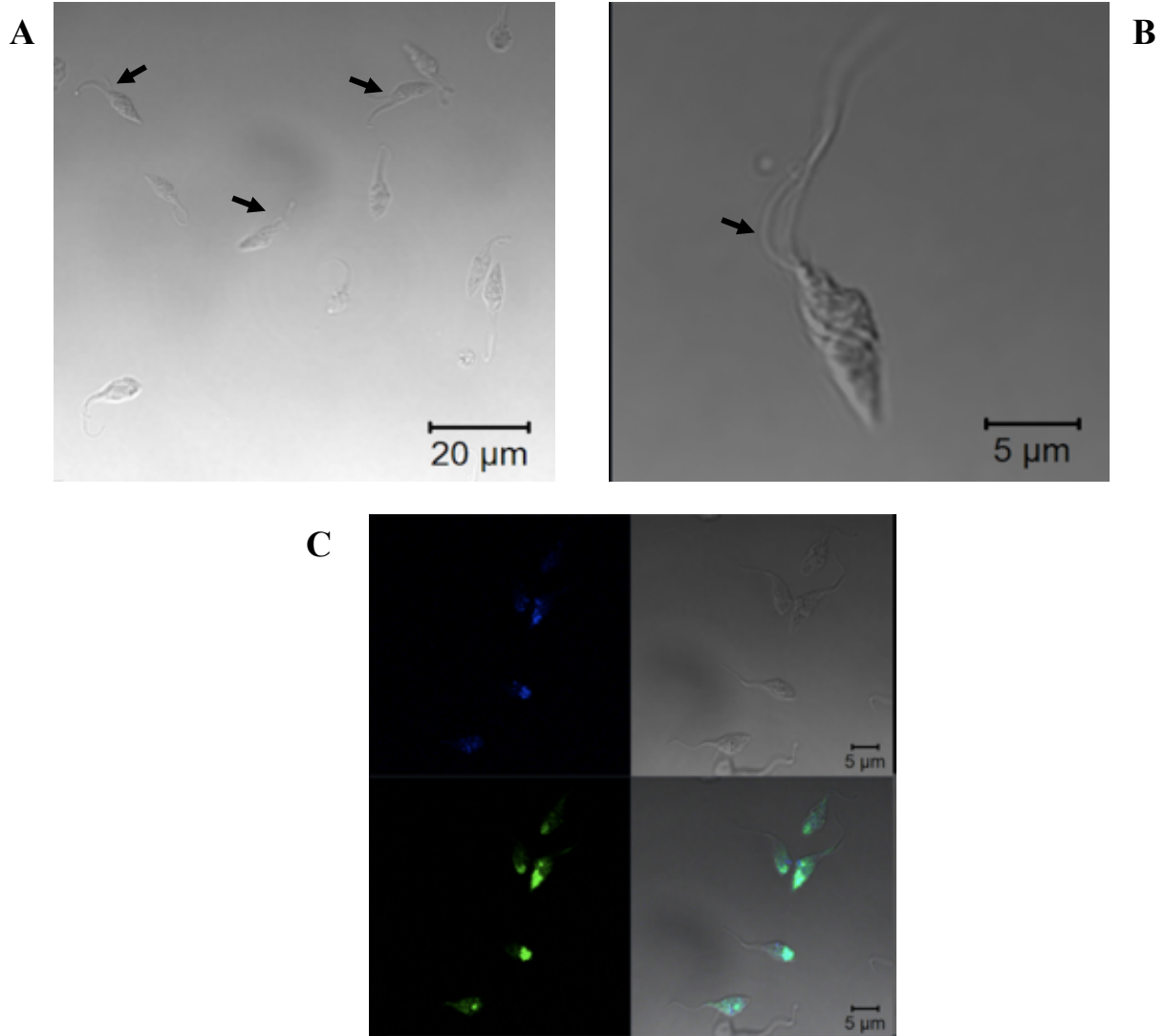


Figure 11. Fluorescence microscopy of PFR2 and UGM *T. cruzi* mutant parasites controlled under the expression of CRISPR/Cas9. (A) Live images of PFR2-KO mutant parasites presenting partial flagellar detachment (arrows). (B) Single PFR2-ablated epimastigote showing detached flagella (arrow). (C) UGM-KO epimastigotes with green fluorescent protein co-localized with DAPI-stained nuclei (blue).

III.5 Generation of *T. cruzi* UGM mutants by CRISPR/Cas9-induced homologous recombination with a selectable marker

In order to repair the double strand break caused by Cas9, we decided to transfect a donor DNA fragment, which consists of a linear cassette with blasticidin flanked by homology arms 100-bp upstream and 100bp-downstream of the start codon, near the Cas9 target site in UGM and PFR2. After co-transfection of pTREX-n/Cas9/sgRNA and donor DNA, mutant cell lines were maintained under double antibiotic selection (neomycin and blasticidin). 8 weeks after, double-resistant cell lines were subjected to PCR analysis. Disruption of UGM was verified using primers that annealed outside the homology regions on the blasticidin cassette, to amplify a fragment from nt -127bp to nt +334bp (**Figure 12A**). A fragment of 666bp corresponded to *T. cruzi*-KO parasites in which the DSB was repaired by homologous recombination, therefore demonstrating DNA disruption. The original fragment, corresponding to WT epimastigotes, represents a fragment of 461bp (**Figure 12C**). Similarly, for our positive control PFR2, previously knocked out by Lander et al., (2015) (56), we used primer annealing outside the homology region of the Bsd cassette to amplify a fragment -142 bp to +234 bp on the PFR2 locus (**Figure 12B**), therefore amplifying a fragment of 696bp in the *T. cruzi*/PFR2-ablated parasites and 376bp in the WT form (**Figure 12C**).

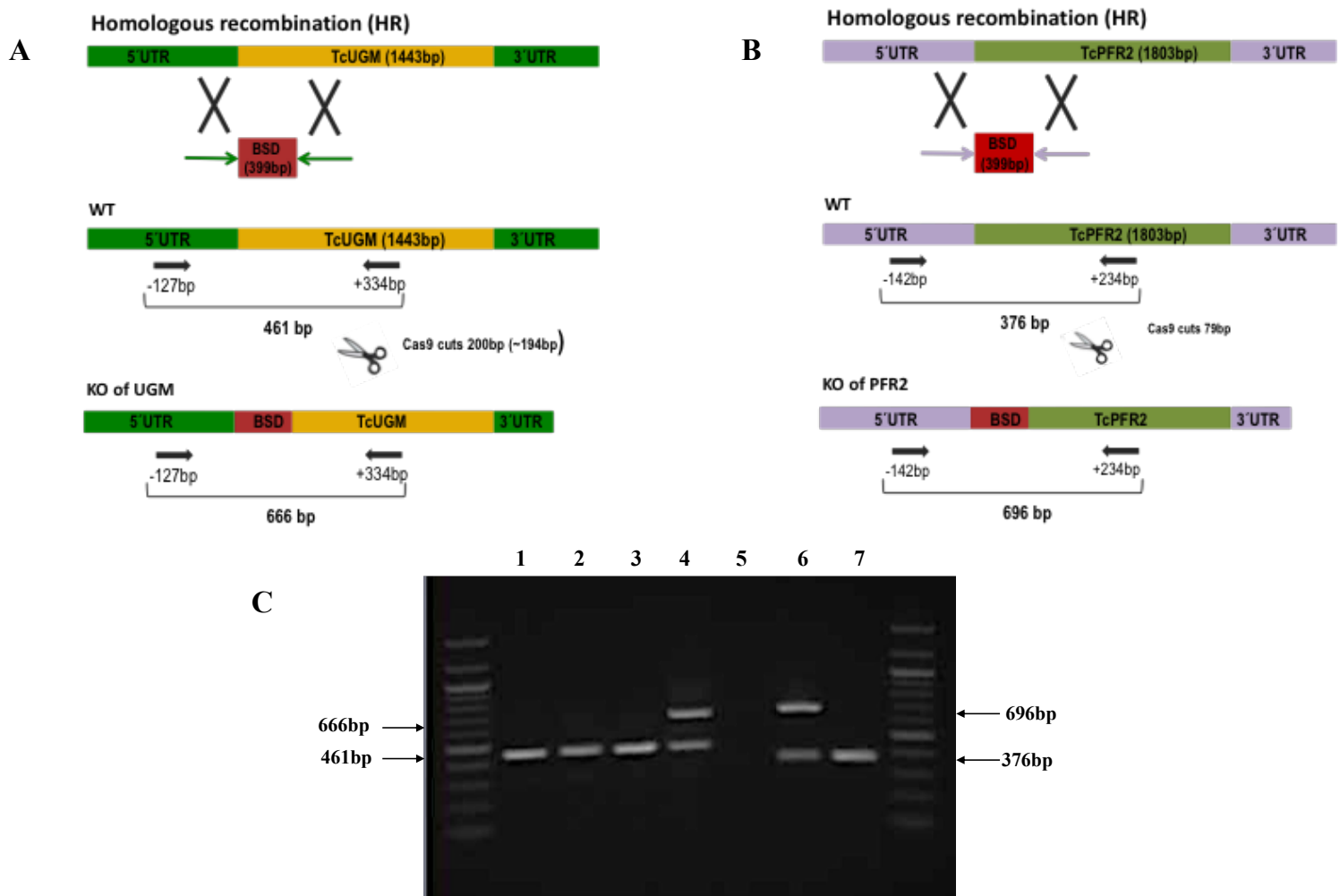


Figure 12. Research strategy used to generate *T. cruzi* UGM and PFR2 mutant parasite by CRISPR/Cas9-induced homologous recombination. (A) Schematic representation of the strategy used to generate *T. cruzi* UGM-KO parasites using homologous recombination to repair the DSB caused by Cas9. A blasticidin-S-deaminase cassette was inserted to repair DNA. Primers annealing outside the homologous regions of the Bsd cassette were designed to amplify a fragment of 461 bp in the intact locus of *T. cruzi* UGM, whereas in the mutant parasite, a fragment of 666 bp was amplified after insertion of Bsd cassette. (B) Strategy used to generate *T. cruzi* PFR2-ablated parasites. Primers outside the homology regions of Bsd were designed to amplify a fragment of 376 bp in WT parasites and 696 bp in mutant parasites. (C) PCR products were obtained from a 1%-agarose gel. Lanes from left to right: 1, UGM WT; 2, UGM pTREX-n/Cas9/sgrscramble RNA (negative control); 3, UGM pTREX-n/Cas9 (negative control); 4, UGM-KO; 5, water control (negative control); 6, PFR2-KO (positive control); 7, PFR2-WT.

Chapter IV: Discussion and future studies

Chagas disease affects approximately 6-8 million people in Latin America, where the disease is mainly endemic. However, recent trends in migration have spread the disease to other countries around the world, such as the U.S, Australia, Japan and Spain, raising an alarm month the public health community. This menacing become important due to its economic burden. Cardiac and digestive complications in the chronic phase of ChD results in an increase of health and treatment cost. Since the majority of the people affected by this disease lives in poor conditions, treatment is often unreachable leading to a high mortality (10). In addition to this, current treatment is highly toxic and partially effective during chronic phase, and there is still no vaccine for ChD. For this reason, it is imperative to study and elucidate the virulence factors of *T. cruzi* and their mechanism of infection, to develop chemotherapeutic drugs for the treatment of ChD (18).

For the last 20 years, *T. cruzi* has been extensively manipulated at the genetic lever in order to better understand its biology. Some of the tools currently available to perform molecular manipulation in *T. cruzi* include integration of expression vectors pRIBOTEX and its derivate pTREX, in which both contain a neomycin selectable marker that is expressed under the Pol I rRNA promoters (58,77). In addition, these expression vectors have been modified by addition of fluorescent protein sequence, such as GFP (green fluorescent protein) and RFP (red fluorescent protein) as a way to monitor parasite infection, through subcellular localization of fused proteins. However, we're still facing limitations in the genetic manipulation of *T. cruzi* (78). Over the past three years, several groups have reported the implementation of the CRISPR/Cas9 systems as a genome editing tool in different parasites such as *P. falciparum* and *Toxoplasma gondii*. In 2015, two separate studies conducted first by Peng et al. (2015), and subsequently Lander and colleagues (2015), demonstrated that CRISPR/Cas9 can be used as an effective way to disrupt genes in *T. cruzi* genome.

Following the ideas established by Lander et al. (2015), here we report the usage of CRISPR/Cas9 system in order to knockout the genes UGM and PFR2, the first potentially involved in the virulence of *T. cruzi* (42) and the second one, in the flagellar development and motility (56). We believe that UGM is not essential for the survival of *T. cruzi*, therefore removal of this gene will not kill the parasites. Here, we introduced the plasmid pTREX-n/Cas9/sgRNA,

along with a blasticidin cassette for homologous recombination into *T. cruzi* (Dm28c) epimastigotes. We chose PFR2 as our positive control, because it was previously demonstrated that disruption of this gene bears flagellar disruption without killing the parasite, as it is appreciated in **Fig. 11B**, therefore making it easy to trace the phenotypic changes caused by Cas9. After 7 weeks of transfection, we PCR mutant parasites both UGM and PFR2, in order to detect insertion of BSD in the site where Cas9 made the double strand break (DSB). The first thing we noticed is that UGM-KO parasites did survive after transfection, therefore demonstrating that indeed this gene is not essential for the survival of *T. cruzi*. We designed a strategy where primers annealing outside the homologous regions of the DSB amplified a fragment of 461 bp in WT UGM epis and 376 bp in WT PFR2 epis, whereas as mutant parasites displayed a fragment of 666 bp in UGM-KO and 696 bp in PFR2-KO epimastigotes. As it is appreciated in **Fig. 12**, both KO-genes present two bands correspond to the WT and KO fragment, therefore suggesting that what we have right now is a mixed population in which some parasites were able to take up the pTREX-n plasmid but not the donor DNA, whereas in other parasites both the plasmid and donor DNA were integrated successfully. What is interesting, is that we should have seen complete disruption of PFR2 as it was previously demonstrated by Lander et al. (2015). In their study, the recovery time after transfection was shorter (5 weeks) and *T. cruzi* PFR2 was completely absent in transfected parasites (56). However, it is important to notice that even though two fragments are amplified in mutant parasites, PFR2-KO shows the fragment corresponding to the WT with less intensity in comparison to the 696-bp fragment; therefore, we believe that WT parasites in the mixed population is less in comparison with the mutant population.

In order to overcome this issue, we will separate these mixed populations for single-cell cloning isolation. Here, we will seed mutant parasites up to a density of 1 parasite/well in conditional media supplemented with different concentrations of blasticidin (250 µg/mL-500 µg/mL) until we can isolate individual clones. As a second strategy, we will cultivate the parasites in semisolid media supplemented with male human urine. A previous study conducted by Fajardo and colleagues (2016), demonstrated that semisolid LIT supplemented with human urine allows for the growth and isolation of *T. cruzi* and *T. brucei* strains from mixed populations cultures in a period of 20 to 30 days approximately (79). From what we have seen from other studies, isolation and manipulation of *T. cruzi* clones requires the usage of limiting dilutions in

order to isolate clonal populations. However, one of the major challenges is that this is time-consuming and the period time to obtain colonies can range up to 30 days or more (76,80). It is possible that the molecular machinery of *T. cruzi* requires more to cause genomic mutations before DNA replication (72).

In summary, our study describes the usage and implementation of the CRISPR/Cas9 machinery as a genome editing tool *T. cruzi*. Here, we were able to generate a plasmid with the 2 main components of CRISPR, the nuclease enzyme Cas9 fused with a GFP marker and our sgRNA. In addition, we were able to introduce antibiotic resistance markers, which overall all of this was able to produce the desired mutations in our parasites. The results and current work of this study represent the efficiency of the CRISPR/Cas9 system as a new tool that can be used to analyze gene function in *T. cruzi*. With this in mind, we hope that this contribution can lead to facilitate genomic studies in the parasite.

References

1. Rassi, A., Jr., Rassi, A., and Marin-Neto, J. A. (2010) Chagas disease. *Lancet* **375**, 1388-1402
2. WHO. (2010) First WHO Report on Neglected Tropical Diseases: Working to Overcome the Global Impact of Neglected Tropical Diseases. . *Geneva: World Health Organization*
3. Bern, C. (2011) Antitrypanosomal therapy for chronic Chagas' disease. *N Engl J Med* **364**, 2527-2534
4. Gascon, J., Bern, C., and Pinazo, M. J. (2010) Chagas disease in Spain, the United States and other non-endemic countries. *Acta Trop* **115**, 22-27
5. Perez-Molina, J. A., and Molina, I. (2018) Chagas disease. *Lancet* **391**, 82-94
6. Requena-Mendez, A., Aldasoro, E., de Lazzari, E., Sicuri, E., Brown, M., Moore, D. A., Gascon, J., and Munoz, J. (2015) Prevalence of Chagas disease in Latin-American migrants living in Europe: a systematic review and meta-analysis. *PLoS Negl Trop Dis* **9**, e0003540
7. Caradonna, K. L., and Burleigh, B. A. (2011) Mechanisms of host cell invasion by *Trypanosoma cruzi*. *Adv Parasitol* **76**, 33-61
8. Barrias, E. S., de Carvalho, T. M., and De Souza, W. (2013) *Trypanosoma cruzi*: Entry into Mammalian Host Cells and Parasitophorous Vacuole Formation. *Front Immunol* **4**, 186
9. Teixeira, D. E., Benchimol, M., Crepaldi, P. H., and de Souza, W. (2012) Interactive multimedia to teach the life cycle of *Trypanosoma cruzi*, the causative agent of Chagas disease. *PLoS Negl Trop Dis* **6**, e1749

10. Nunes, M. C., Dones, W., Morillo, C. A., Encina, J. J., Ribeiro, A. L., and Council on Chagas Disease of the Interamerican Society of, C. (2013) Chagas disease: an overview of clinical and epidemiological aspects. *J Am Coll Cardiol* **62**, 767-776
11. Noya, B. A., Diaz-Bello, Z., Colmenares, C., Ruiz-Guevara, R., Mauriello, L., Munoz-Calderon, A., and Noya, O. (2015) Update on oral Chagas disease outbreaks in Venezuela: epidemiological, clinical and diagnostic approaches. *Mem Inst Oswaldo Cruz* **110**, 377-386
12. Bern, C., Kjos, S., Yabsley, M. J., and Montgomery, S. P. (2011) Trypanosoma cruzi and Chagas' Disease in the United States. *Clin Microbiol Rev* **24**, 655-681
13. Bonney, K. M. (2014) Chagas disease in the 21st century: a public health success or an emerging threat? *Parasite* **21**, 11
14. Carod-Artal, F. J., and Gascon, J. (2010) Chagas disease and stroke. *Lancet Neurol* **9**, 533-542
15. Cardoso, R. N., Macedo, F. Y., Garcia, M. N., Garcia, D. C., Benjo, A. M., Aguilar, D., Jneid, H., and Bozkurt, B. (2014) Chagas cardiomyopathy is associated with higher incidence of stroke: a meta-analysis of observational studies. *J Card Fail* **20**, 931-938
16. Ciapponi, A., Alcaraz, A., Calderon, M., Matta, M. G., Chaparro, M., Soto, N., and Bardach, A. (2016) Burden of Heart Failure in Latin America: A Systematic Review and Meta-analysis. *Rev Esp Cardiol (Engl Ed)* **69**, 1051-1060
17. Release, F. N. (2017) FDA approves first U.S. treatment for Chagas disease.
18. Urbina, J. A. (2010) Specific chemotherapy of Chagas disease: relevance, current limitations and new approaches. *Acta Trop* **115**, 55-68

19. Urbina, J. A. (2015) Recent clinical trials for the etiological treatment of chronic chagas disease: advances, challenges and perspectives. *J Eukaryot Microbiol* **62**, 149-156
20. Torrico, F., Gascon, J., Ortiz, L., Alonso-Vega, C., Pinazo, M. J., Schijman, A., Almeida, I. C., Alves, F., Strub-Wourgaft, N., Ribeiro, I., and Group, E. S. (2018) Treatment of adult chronic indeterminate Chagas disease with benznidazole and three E1224 dosing regimens: a proof-of-concept, randomised, placebo-controlled trial. *Lancet Infect Dis* **18**, 419-430
21. Viotti, R., Alarcon de Noya, B., Araujo-Jorge, T., Grijalva, M. J., Guhl, F., Lopez, M. C., Ramsey, J. M., Ribeiro, I., Schijman, A. G., Sosa-Estani, S., Torrico, F., Gascon, J., and Latin American Network for Chagas Disease, N. (2014) Towards a paradigm shift in the treatment of chronic Chagas disease. *Antimicrob Agents Chemother* **58**, 635-639
22. Dumonteil, E., Bottazzi, M. E., Zhan, B., Heffernan, M. J., Jones, K., Valenzuela, J. G., Kamhawi, S., Ortega, J., de Leon Rosales, S. P., Lee, B. Y., Bacon, K. M., Fleischer, B., Slingsby, B. T., Cravioto, M. B., Tapia-Conyer, R., and Hotez, P. J. (2012) Accelerating the development of a therapeutic vaccine for human Chagas disease: rationale and prospects. *Expert Rev Vaccines* **11**, 1043-1055
23. Hotez, P. J., Bottazzi, M. E., and Strych, U. (2016) New Vaccines for the World's Poorest People. *Annu Rev Med* **67**, 405-417
24. Rodriguez-Morales, O., Monteon-Padilla, V., Carrillo-Sanchez, S. C., Rios-Castro, M., Martinez-Cruz, M., Carabarin-Lima, A., and Arce-Fonseca, M. (2015) Experimental Vaccines against Chagas Disease: A Journey through History. *J Immunol Res* **2015**, 489758

25. Schneider, P., Rosat, J. P., Ransijn, A., Ferguson, M. A., and McConville, M. J. (1993) Characterization of glycoinositol phospholipids in the amastigote stage of the protozoan parasite *Leishmania major*. *Biochem J* **295** (Pt 2), 555-564
26. Kinoshita, T., and Fujita, M. (2016) Biosynthesis of GPI-anchored proteins: special emphasis on GPI lipid remodeling. *J Lipid Res* **57**, 6-24
27. Almeida, I. C., and Gazzinelli, R. T. (2001) Proinflammatory activity of glycosylphosphatidylinositol anchors derived from *Trypanosoma cruzi*: structural and functional analyses. *J Leukoc Biol* **70**, 467-477
28. Acosta-Serrano, A., Hutchinson, C., Nakayasu, E. S., Almeida, I. C., and Carrington, M. (2007) Comparison and evolution of the surface architecture of trypanosomatid parasites. in *Trypanosomes: After the genome* (Barry, J. D., Mottram, J. C., McCulloch, R., and Acosta-Serrano, A. eds.), Horizon Scientific Press, Norwich, UK. pp 319-337
29. Ferguson, M. A. (1997) The surface glycoconjugates of trypanosomatid parasites. *Philos Trans R Soc Lond B Biol Sci* **352**, 1295-1302
30. Mendonca-Previato, L., Todeschini, A. R., Heise, N., and Previato, J. O. (2005) Protozoan parasite-specific carbohydrate structures. *Curr Opin Struct Biol* **15**, 499-505
31. Pereira-Chiocola, V. L., Acosta-Serrano, A., Correia de Almeida, I., Ferguson, M. A., Souto-Padron, T., Rodrigues, M. M., Travassos, L. R., and Schenkman, S. (2000) Mucin-like molecules form a negatively charged coat that protects *Trypanosoma cruzi* trypomastigotes from killing by human anti-alpha-galactosyl antibodies. *J Cell Sci* **113** (Pt 7), 1299-1307
32. de Lederkremer, R. M., and Agusti, R. (2009) Glycobiology of *Trypanosoma cruzi*. *Adv Carbohydr Chem Biochem* **62**, 311-366

33. de Lederkremer, R. M., and Colli, W. (1995) Galactofuranose-containing glycoconjugates in trypanosomatids. *Glycobiology* **5**, 547-552
34. Richards, M. R., and Lowary, T. L. (2009) Chemistry and biology of galactofuranose-containing polysaccharides. *Chembiochem* **10**, 1920-1938
35. McConville, M. J., and Ferguson, M. A. (1993) The structure, biosynthesis and function of glycosylated phosphatidylinositols in the parasitic protozoa and higher eukaryotes. *Biochem J* **294** (Pt 2), 305-324
36. Branquinha, M. H., Vermelho, A. B., Almeida, I. C., Mehlert, A., and Ferguson, M. A. (1999) Structural studies on the polar glycoinositol phospholipids of *Trypanosoma* (*Schizotrypanum*) *dionisii* from bats. *Mol Biochem Parasitol* **102**, 179-189
37. Mendonca-Previato, L., Penha, L., Garcez, T. C., Jones, C., and Previato, J. O. (2013) Addition of alpha-O-GlcNAc to threonine residues define the post-translational modification of mucin-like molecules in *Trypanosoma cruzi*. *Glycoconj J* **30**, 659-666
38. Serrano, A. A., Schenkman, S., Yoshida, N., Mehlert, A., Richardson, J. M., and Ferguson, M. A. (1995) The lipid structure of the glycosylphosphatidylinositol-anchored mucin-like sialic acid acceptors of *Trypanosoma cruzi* changes during parasite differentiation from epimastigotes to infective metacyclic trypomastigote forms. *J Biol Chem* **270**, 27244-27253
39. Zingales, B., Miles, M. A., Campbell, D. A., Tibayrenc, M., Macedo, A. M., Teixeira, M. M., Schijman, A. G., Llewellyn, M. S., Lages-Silva, E., Machado, C. R., Andrade, S. G., and Sturm, N. R. (2012) The revised *Trypanosoma cruzi* subspecific nomenclature: rationale, epidemiological relevance and research applications. *Infection, genetics and*

evolution : journal of molecular epidemiology and evolutionary genetics in infectious diseases **12**, 240-253

40. Carreira, J. C., Jones, C., Wait, R., Previato, J. O., and Mendonca-Previato, L. (1996) Structural variation in the glycoinositolphospholipids of different strains of *Trypanosoma cruzi*. *Glycoconj J* **13**, 955-966
41. Golgher, D. B., Colli, W., Souto-Padron, T., and Zingales, B. (1993) Galactofuranose-containing glycoconjugates of epimastigote and trypomastigote forms of *Trypanosoma cruzi*. *Mol Biochem Parasitol* **60**, 249-264
42. Oppenheimer, M., Valenciano, A. L., and Sobrado, P. (2011) Biosynthesis of galactofuranose in kinetoplastids: novel therapeutic targets for treating leishmaniasis and chagas' disease. *Enzyme Res* **2011**, 415976
43. Nogueira, N. F., Gonzalez, M. S., Gomes, J. E., de Souza, W., Garcia, E. S., Azambuja, P., Nohara, L. L., Almeida, I. C., Zingales, B., and Colli, W. (2007) *Trypanosoma cruzi*: involvement of glycoinositolphospholipids in the attachment to the luminal midgut surface of *Rhodnius prolixus*. *Exp Parasitol* **116**, 120-128
44. Tanner, J. J., Boechi, L., Andrew McCammon, J., and Sobrado, P. (2014) Structure, mechanism, and dynamics of UDP-galactopyranose mutase. *Arch Biochem Biophys* **544**, 128-141
45. Nassau, P. M., Martin, S. L., Brown, R. E., Weston, A., Monsey, D., McNeil, M. R., and Duncan, K. (1996) Galactofuranose biosynthesis in *Escherichia coli* K-12: identification and cloning of UDP-galactopyranose mutase. *J Bacteriol* **178**, 1047-1052

46. Beverley, S. M., Owens, K. L., Showalter, M., Griffith, C. L., Doering, T. L., Jones, V. C., and McNeil, M. R. (2005) Eukaryotic UDP-galactopyranose mutase (GLF gene) in microbial and metazoal pathogens. *Eukaryot Cell* **4**, 1147-1154
47. Oppenheimer, M., Valenciano, A. L., Kizjakina, K., Qi, J., and Sobrado, P. (2012) Chemical mechanism of UDP-galactopyranose mutase from *Trypanosoma cruzi*: a potential drug target against Chagas' disease. *PLoS One* **7**, e32918
48. Pan, F., Jackson, M., Ma, Y., and McNeil, M. (2001) Cell wall core galactofuran synthesis is essential for growth of mycobacteria. *J Bacteriol* **183**, 3991-3998
49. Schmalhorst, P. S., Krappmann, S., Vervecken, W., Rohde, M., Muller, M., Braus, G. H., Contreras, R., Braun, A., Bakker, H., and Routier, F. H. (2008) Contribution of galactofuranose to the virulence of the opportunistic pathogen *Aspergillus fumigatus*. *Eukaryot Cell* **7**, 1268-1277
50. Engel, J., Schmalhorst, P. S., Dork-Bousset, T., Ferrieres, V., and Routier, F. H. (2009) A single UDP-galactofuranose transporter is required for galactofuranosylation in *Aspergillus fumigatus*. *J Biol Chem* **284**, 33859-33868
51. Kleczka, B., Lamerz, A. C., van Zandbergen, G., Wenzel, A., Gerardy-Schahn, R., Wiese, M., and Routier, F. H. (2007) Targeted gene deletion of *Leishmania major* UDP-galactopyranose mutase leads to attenuated virulence. *J Biol Chem* **282**, 10498-10505
52. Dhatwalia, R., Singh, H., Oppenheimer, M., Sobrado, P., and Tanner, J. J. (2012) Crystal structures of *Trypanosoma cruzi* UDP-galactopyranose mutase implicate flexibility of the histidine loop in enzyme activation. *Biochemistry* **51**, 4968-4979
53. El-Sayed, N. M., Myler, P. J., Bartholomeu, D. C., Nilsson, D., Aggarwal, G., Tran, A. N., Ghedin, E., Worthey, E. A., Delcher, A. L., Blandin, G., Westenberger, S. J., Caler, H. J., et al. (2007) The genome of *Trypanosoma brucei*. *Nature* **450**, 101-108

- E., Cerqueira, G. C., Branche, C., Haas, B., Anupama, A., Arner, E., Aslund, L., Attipoe, P., Bontempi, E., Bringaud, F., Burton, P., Cadag, E., Campbell, D. A., Carrington, M., Crabtree, J., Darban, H., da Silveira, J. F., de Jong, P., Edwards, K., Englund, P. T., Fazelina, G., Feldblyum, T., Ferella, M., Frasch, A. C., Gull, K., Horn, D., Hou, L., Huang, Y., Kindlund, E., Klingbeil, M., Kluge, S., Koo, H., Lacerda, D., Levin, M. J., Lorenzi, H., Louie, T., Machado, C. R., McCulloch, R., McKenna, A., Mizuno, Y., Mottram, J. C., Nelson, S., Ochaya, S., Osoegawa, K., Pai, G., Parsons, M., Pentony, M., Pettersson, U., Pop, M., Ramirez, J. L., Rinta, J., Robertson, L., Salzberg, S. L., Sanchez, D. O., Seyler, A., Sharma, R., Shetty, J., Simpson, A. J., Sisk, E., Tammi, M. T., Tarleton, R., Teixeira, S., Van Aken, S., Vogt, C., Ward, P. N., Wickstead, B., Wortman, J., White, O., Fraser, C. M., Stuart, K. D., and Andersson, B. (2005) The genome sequence of *Trypanosoma cruzi*, etiologic agent of Chagas disease. *Science* **309**, 409-415
54. Batista, M., Marchini, F. K., Celedon, P. A., Fragoso, S. P., Probst, C. M., Preti, H., Ozaki, L. S., Buck, G. A., Goldenberg, S., and Krieger, M. A. (2010) A high-throughput cloning system for reverse genetics in *Trypanosoma cruzi*. *BMC Microbiol* **10**, 259
 55. Docampo, R. (2011) Molecular parasitology in the 21st century. *Essays Biochem* **51**, 1-13
 56. Lander, N., Li, Z. H., Niyogi, S., and Docampo, R. (2015) CRISPR/Cas9-Induced Disruption of Paraflagellar Rod Protein 1 and 2 Genes in *Trypanosoma cruzi* Reveals Their Role in Flagellar Attachment. *MBio* **6**, e01012
 57. Taylor, M. C., Huang, H., and Kelly, J. M. (2011) Genetic techniques in *Trypanosoma cruzi*. *Adv Parasitol* **75**, 231-250
 58. Lorenzi, H. A., Vazquez, M. P., and Levin, M. J. (2003) Integration of expression vectors into the ribosomal locus of *Trypanosoma cruzi*. *Gene* **310**, 91-99

59. Hofflin, J. M., Sadler, R. H., Araujo, F. G., Page, W. E., and Remington, J. S. (1987) Laboratory-acquired Chagas disease. *Trans R Soc Trop Med Hyg* **81**, 437-440
60. Lander, N., Chiurillo, M. A., and Docampo, R. (2016) Genome Editing by CRISPR/Cas9: A Game Change in the Genetic Manipulation of Protists. *J Eukaryot Microbiol* **63**, 679-690
61. Doudna, J. A., and Charpentier, E. (2014) Genome editing. The new frontier of genome engineering with CRISPR-Cas9. *Science* **346**, 1258096
62. Ishino, Y., Shinagawa, H., Makino, K., Amemura, M., and Nakata, A. (1987) Nucleotide sequence of the iap gene, responsible for alkaline phosphatase isozyme conversion in *Escherichia coli*, and identification of the gene product. *J Bacteriol* **169**, 5429-5433
63. Makarova, K. S., Haft, D. H., Barrangou, R., Brouns, S. J., Charpentier, E., Horvath, P., Moineau, S., Mojica, F. J., Wolf, Y. I., Yakunin, A. F., van der Oost, J., and Koonin, E. V. (2011) Evolution and classification of the CRISPR-Cas systems. *Nat Rev Microbiol* **9**, 467-477
64. Garneau, J. E., Dupuis, M. E., Villion, M., Romero, D. A., Barrangou, R., Boyaval, P., Fremaux, C., Horvath, P., Magadan, A. H., and Moineau, S. (2010) The CRISPR/Cas bacterial immune system cleaves bacteriophage and plasmid DNA. *Nature* **468**, 67-71
65. Horvath, P., and Barrangou, R. (2010) CRISPR/Cas, the immune system of bacteria and archaea. *Science* **327**, 167-170
66. Jinek, M., Chylinski, K., Fonfara, I., Hauer, M., Doudna, J. A., and Charpentier, E. (2012) A programmable dual-RNA-guided DNA endonuclease in adaptive bacterial immunity. *Science* **337**, 816-821

67. Sander, J. D., and Joung, J. K. (2014) CRISPR-Cas systems for editing, regulating and targeting genomes. *Nat Biotechnol* **32**, 347-355
68. Makarova, K. S., Wolf, Y. I., Alkhnbashi, O. S., Costa, F., Shah, S. A., Saunders, S. J., Barrangou, R., Brouns, S. J., Charpentier, E., Haft, D. H., Horvath, P., Moineau, S., Mojica, F. J., Terns, R. M., Terns, M. P., White, M. F., Yakunin, A. F., Garrett, R. A., van der Oost, J., Backofen, R., and Koonin, E. V. (2015) An updated evolutionary classification of CRISPR-Cas systems. *Nat Rev Microbiol* **13**, 722-736
69. van der Oost, J., Westra, E. R., Jackson, R. N., and Wiedenheft, B. (2014) Unravelling the structural and mechanistic basis of CRISPR-Cas systems. *Nat Rev Microbiol* **12**, 479-492
70. Deltcheva, E., Chylinski, K., Sharma, C. M., Gonzales, K., Chao, Y., Pirzada, Z. A., Eckert, M. R., Vogel, J., and Charpentier, E. (2011) CRISPR RNA maturation by trans-encoded small RNA and host factor RNase III. *Nature* **471**, 602-607
71. Ran, F. A., Hsu, P. D., Wright, J., Agarwala, V., Scott, D. A., and Zhang, F. (2013) Genome engineering using the CRISPR-Cas9 system. *Nat Protoc* **8**, 2281-2308
72. Peng, D., Kurup, S. P., Yao, P. Y., Minning, T. A., and Tarleton, R. L. (2014) CRISPR-Cas9-mediated single-gene and gene family disruption in *Trypanosoma cruzi*. *MBio* **6**, e02097-02014
73. Lander, N., Chiurillo, M. A., Storey, M., Vercesi, A. E., and Docampo, R. (2016) CRISPR/Cas9-mediated endogenous C-terminal Tagging of *Trypanosoma cruzi* Genes Reveals the Acidocalcisome Localization of the Inositol 1,4,5-Trisphosphate Receptor. *J Biol Chem* **291**, 25505-25515

74. Camargo, E. P. (1964) Growth and Differentiation in Trypanosoma Cruzi. I. Origin of Metacyclic Trypanosomes in Liquid Media. *Rev Inst Med Trop Sao Paulo* **6**, 93-100
75. Peng, D., and Tarleton, R. (2015) EuPaGDT: a web tool tailored to design CRISPR guide RNAs for eukaryotic pathogens. *Microb Genom* **1**, e000033
76. Bouvier, L. A., Camara Mde, L., Canepa, G. E., Miranda, M. R., and Pereira, C. A. (2013) Plasmid vectors and molecular building blocks for the development of genetic manipulation tools for Trypanosoma cruzi. *PLoS One* **8**, e80217
77. Vazquez, M. P., and Levin, M. J. (1999) Functional analysis of the intergenic regions of TcP2beta gene loci allowed the construction of an improved Trypanosoma cruzi expression vector. *Gene* **239**, 217-225
78. Burle-Caldas Gde, A., Grazielle-Silva, V., Laibida, L. A., DaRocha, W. D., and Teixeira, S. M. (2015) Expanding the tool box for genetic manipulation of Trypanosoma cruzi. *Mol Biochem Parasitol* **203**, 25-33
79. Fajardo, E. F., Cabrine-Santos, M., Ferreira, K. A., Lages-Silva, E., Ramirez, L. E., and Pedrosa, A. L. (2016) Semisolid liver infusion tryptose supplemented with human urine allows growth and isolation of Trypanosoma cruzi and Trypanosoma rangeli clonal lineages. *Rev Soc Bras Med Trop* **49**, 369-372
80. Xu, D., Brandan, C. P., Basombrio, M. A., and Tarleton, R. L. (2009) Evaluation of high efficiency gene knockout strategies for Trypanosoma cruzi. *BMC Microbiol* **9**, 90

Vita

Claudia Manríquez-Román was born and raised in Ciudad Juarez, Mexico. Around the time she graduated from high school, Juarez became the stage of a very violent war on drugs that led her to pursue a better education outside Mexico. Committed to take a long commute from Juarez to El Paso, TX daily, Claudia earned her Bachelor of Science in Microbiology from the University of Texas at EL Paso (UTEP) in 2016.

As an undergraduate student, Claudia was trained in the area of parasitology under the mentorship of Rosa Maldonado, PhD. For 2 years she worked on her project titled “Evaluation of Chagas disease in wild and domestic reservoirs in El Paso County”, to which she qualified to receive funding from the UTEP’S Campus of Undergraduate Research Initiatives (COURI) program. In 2016, Claudia was accepted into the Master of Science program at UTEP under the leadership of Dr. Igor C. Almeida, where she has been extensively trained in the area of molecular parasitology. During her journey as a master’s student, Claudia has developed many skills involving critical interpretation of scientific literature and mentoring undergraduate, all of which have served as the foundation in becoming a strong scholarly researcher.

Finally, Claudia will begin her Ph.D. at the Mayo Clinic where she was granted the 2017 Dean’s Fellowship under the Virology and Gene Therapy Program.

This thesis was typed by Claudia Manriquez-Roman